Neuroscience

Inhibitory CCK+ basket synapse defects in mouse models of dystroglycanopathy

Reviewed Preprint

Revised by authors after peer review.

About eLife's process

Reviewed preprint version 2
November 22, 2023 (this version)

Reviewed preprint version 1
May 17, 2023

Sent for peer review
March 27, 2023

Posted to bioRxiv
February 28, 2023

Jennifer N. Jahncke, Daniel S. Miller, Milana Krush, Eric Schnell, Kevin M. Wright

Neuroscience Graduate Program, Oregon Health & Science University, Portland, OR 97239, USA • Operative Care Division, Portland VA Health Care System • Anesthesiology and Perioperative Medicine, Oregon Health & Science University, Portland, OR 97239, USA • Vollum Institute, Oregon Health & Science University, Portland, OR 97239, USA

Abstract

Dystroglycan (Dag1) is a transmembrane glycoprotein that links the extracellular matrix to the actin cytoskeleton. Mutations in *Dag1* or the genes required for its glycosylation result in dystroglycanopathy, a type of congenital muscular dystrophy characterized by a wide range of phenotypes including muscle weakness, brain defects, and cognitive impairment. We investigated interneuron (IN) development, synaptic function, and associated seizure susceptibility in multiple mouse models that reflect the wide phenotypic range of dystroglycanopathy neuropathology. Mice that model severe dystroglycanopathy due to forebrain deletion of *Dag1* or *Pomt2*, which is required for Dystroglycan glycosylation, show significant impairment of $CCK^+/CB1R^+$ IN development. $CCK^+/CB1R^+$ IN axons failed to properly target the somatodendritic compartment of pyramidal neurons in the hippocampus, resulting in synaptic defects and increased seizure susceptibility. Mice lacking the intracellular domain of Dystroglycan have milder defects in $CCK^+/CB1R^+$ IN axon targeting, but exhibit dramatic changes in inhibitory synaptic function, indicating a critical postsynaptic role of this domain. In contrast, $CCK^+/CB1R^+$ IN synaptic function and seizure susceptibility was normal in mice that model mild dystroglycanopathy due to partially reduced Dystroglycan glycosylation. Collectively, these data show that inhibitory synaptic defects and elevated seizure susceptibility are hallmarks of severe dystroglycanopathy, and show that Dystroglycan plays an important role in organizing functional inhibitory synapse assembly.

eLife assessment

These **important** findings will be of interest for the study of dystroglycanopathies and in the general area of axon migration and synapse formation. This work provides **convincing** conclusions about how a range of dystroglycan mutations alter CCK interneuron axonal targeting and synaptic connectivity in the forebrain, and seizure susceptibility.

Introduction

The formation of neural circuits is a multistep process involving proliferation, migration, axon guidance, maturation of neuronal subtypes, and establishment of functional synaptic connections between neurons. The cell adhesion molecule Dystroglycan is widely expressed in muscle and brain. Within the forebrain, Dystroglycan is expressed in neuroepithelial cells, pyramidal neurons, astrocytes, oligodendrocytes, and vascular endothelial cells where it plays important roles in the formation of basement membranes during early brain development (Colognato et al., 2007; Nguyen et al., 2014; Nickolls & Bönnemann, 2018; Tian et al., 1996; Zaccaria et al., 2001). At later developmental stages, Dystroglycan is present at multiple synapses, including at photoreceptor ribbon synapses in the retina (Omori et al., 2012; Orlandi et al., 2018), inhibitory synapses in the cerebellum (Briatore et al., 2010, 2020; Patrizi et al., 2008), and inhibitory synapses onto pyramidal neurons (Brünig et al., 2002; Lévi et al., 2002).

Dystroglycan is a central component of the dystrophin-glycoprotein complex (DGC) known primarily for its role in the etiology of neuromuscular diseases including Duchenne muscular dystrophy (DMD), limb-girdle muscular dystrophy (LGMD), and congenital muscular dystrophy (CMD). The gene encoding *Dystroglycan* (*Dag1*) yields two subunits, the extracellular alpha Dystroglycan (α-Dag1) and the transmembrane beta Dystroglycan (β-Dag1). These two subunits are non-covalently bound, allowing Dystroglycan to function as a link between extracellular ligands and cytoskeletal and signaling proteins (Ervasti & Campbell, 1991; Holt et al., 2000; Ibraghimov-Beskrovnaya et al., 1992; C. J. Moore & Winder, 2010). Extracellular α-Dag1 interacts with multiple proteins in the nervous system through its extensive glycan chains (Jahncke & Wright, 2023). Mutations in any of the 19 genes involved in α-Dag1 glycosylation impair Dystroglycan function through reduced ligand binding and leads to a class of congenital muscular dystrophy termed dystroglycanopathy (Blaeser et al., 2013). Patients with severe forms of dystroglycanopathy frequently present with structural brain abnormalities and experience seizures and cognitive impairments (Barresi & Campbell, 2006; Muntoni et al., 2011; Taniguchi-Ikeda et al., 2016). Dystroglycanopathy patients with moderate severity can exhibit cognitive impairments even in the absence of identifiable brain malformations, suggesting that Dystroglycan functions at later stages of neural circuit formation such as synapse formation and/or maintenance (Clement et al., 2008; Godfrey et al., 2007).

The dramatic structural and anatomical phenotypes of global *Dag1* deletion in mice has often precluded analysis of Dystroglycan's synaptic functions (Myshrall et al., 2012; Satz et al., 2008, 2010). Recent studies show that when *Dag1* is selectively deleted from postmitotic pyramidal neurons, neuronal migration and lamination is normal, however $CCK^+/CB1R^+$ interneurons (INs) fail to populate the forebrain or form synapses in these mice (Früh et al., 2016; Miller & Wright, 2021). Furthermore, conditional deletion of *Dag1* from cerebellar Purkinje neurons leads to impaired inhibitory synaptic transmission and a reduction in the number of inhibitory synapses in cerebellar cortex (Briatore et al., 2020). These studies establish a role for Dystroglycan function at a subset of inhibitory synapses in the brain, but the critical features of Dystroglycan necessary for these functions, and the relationship between inhibitory synaptogenesis and neurological phenotypes in dystroglycanopathy, remains undefined.

Here, we use multiple mouse models that recapitulate the full range of dystroglycanopathy neuropathology to address several outstanding questions related to the role of Dystroglycan at inhibitory synapses. We find that $CCK^+/CB1R^+$ IN axon targeting, synapse formation, and synapse function requires both glycosylation of α- Dag1 and interactions through the intracellular domain of β-Dag1, and that defects in synaptic structure and function is associated with increased seizure susceptibility in mouse models of dystroglycanopathy.

Results

Characterizing Dystroglycan localization and glycosylation in multiple models of dystroglycanopathy

While conditional deletion of *Dag1* from pyramidal neurons causes a loss of CCK^+/$CB1R^+$ IN innervation in the forebrain, this has not been examined in dystroglycanopathy relevant mouse models exhibiting more widespread loss of functional Dystroglycan. We therefore generated five distinct mouse models; three to provide mechanistic insight into Dystroglycan function and two of which model mild dystroglycanopathy (schematized in **Fig. 1A**). Since complete loss of *Dag1* results in early embryonic lethality in mice, we generated forebrain-specific conditional knockouts by crossing $Emx1^{Cre}$ with *Dystroglycan* floxed mice ($Dag1^{F/F}$), to drive recombination in neuroepithelial cells in the dorsal forebrain beginning at embryonic day 10.5 (E10.5) (Gorski et al., 2002; Liang et al., 2012). We verified the recombination pattern of $Emx1^{Cre}$ with the mCherry reporter $Rosa26^{Lox\text{-}STOP\text{-}Lox\text{-}H2B:mCherry}$. H2B:mCherry signal was present in all excitatory neurons and astrocytes throughout the forebrain (**Fig. 1 Supp. 1A, B, D**) but not microglia or interneurons (**Fig. 1 Supp. 1C, E**).

To model loss of Dystroglycan glycosylation, $Emx1^{Cre}$was crossed with $Pomt2^{F/F}$ conditional mice to generate $Pomt2^{cKOs}$. Pomt2 (protein *O*-mannosyltransferase 2) is a glycosyltransferase that functions in a heterocomplex with Pomt1 to add *O*-mannose at the beginning of the Dystroglycan glycan chain (Manya et al., 2004). Without the initial *O*-mannose, no additional sugar moieties can be added to the glycan chain, resulting in near complete loss of Dystroglycan glycosylation. This is lethal embryonically in a global *Pomt2* knockout, however $Emx1^{Cre}$;$Pomt2^{cKO}$ mice are viable and survive into adulthood (Hu et al., 2016; Reeuwijk et al., 2005; Yanagisawa et al., 2007).

In addition to binding extracellular ligands, Dystroglycan binds cytoskeletal proteins and signals through the intracellular tail of its β-subunit. To determine whether the intracellular domain of Dystroglycan is required for synaptic development and/or function, we examined mice in which one copy of *Dag1* was deleted, and the other copy lacks the intracellular domain of β-Dag1 ($Dag1^{cyto/-}$). These mice develop muscular dystrophy but show normal neuronal migration and axon guidance in regions throughout the central nervous system where Dystroglycan glycosylation is required (Lindenmaier et al., 2019; Satz et al., 2009, 2010).

To model mild forms of dystroglycanopathy, we examined mice expressing missense mutations in *B4gat1 (*β-1,4-glucuronyltransferase, $B4gat1^{M155T}$) and *Fkrp* (fukutin related protein, $Fkrp^{P448L}$), two genes required for Dystroglycan glycosylation. $B4gat1^{M155T}$ mice were initially identified in a forward genetic screen and develop mild muscular dystrophy and have diminished ligand binding capacity due to reduced Dystroglycan glycosylation (Wright et al., 2012). The $Fkrp^{P448L}$missense mutation models a mutation found in a patient with dystroglycanopathy (Brockington et al., 2001). In mice, the $Fkrp^{P448L}$mutation leads to reduced glycosylation and mild muscular dystrophy, but no gross brain or eye malformations (Blaeser et al., 2013). While it is possible that *Pomt2*, *B4gat1*, and *Fkrp* could play a role in the glycosylation of proteins other than Dystroglycan, the identity of these proteins has not been described in neurons to date and we did not observe any emergent phenotypes that have not been observed in *Dag1* mutants (Gerin et al., 2016; Larsen, Narimatsu, Joshi, Siukstaite, et al., 2017; Larsen, Narimatsu, Joshi, Yang, et al., 2017; Willer et al., 2014).

We first examined the pattern of Dystroglycan localization in pyramidal neurons in CA1 of hippocampus in each of the five models by immunostaining adult (P30) mice with the IIH6 antibody, which detects the terminal matriglycan repeats on the glycan chain on α-Dag1 (Sheikh et al., 2022; Yoshida-Moriguchi & Campbell, 2015). In wild-type (WT) mice, punctate IIH6 immunoreactivity was evident in the somatic and perisomatic compartment of CA1 pyramidal

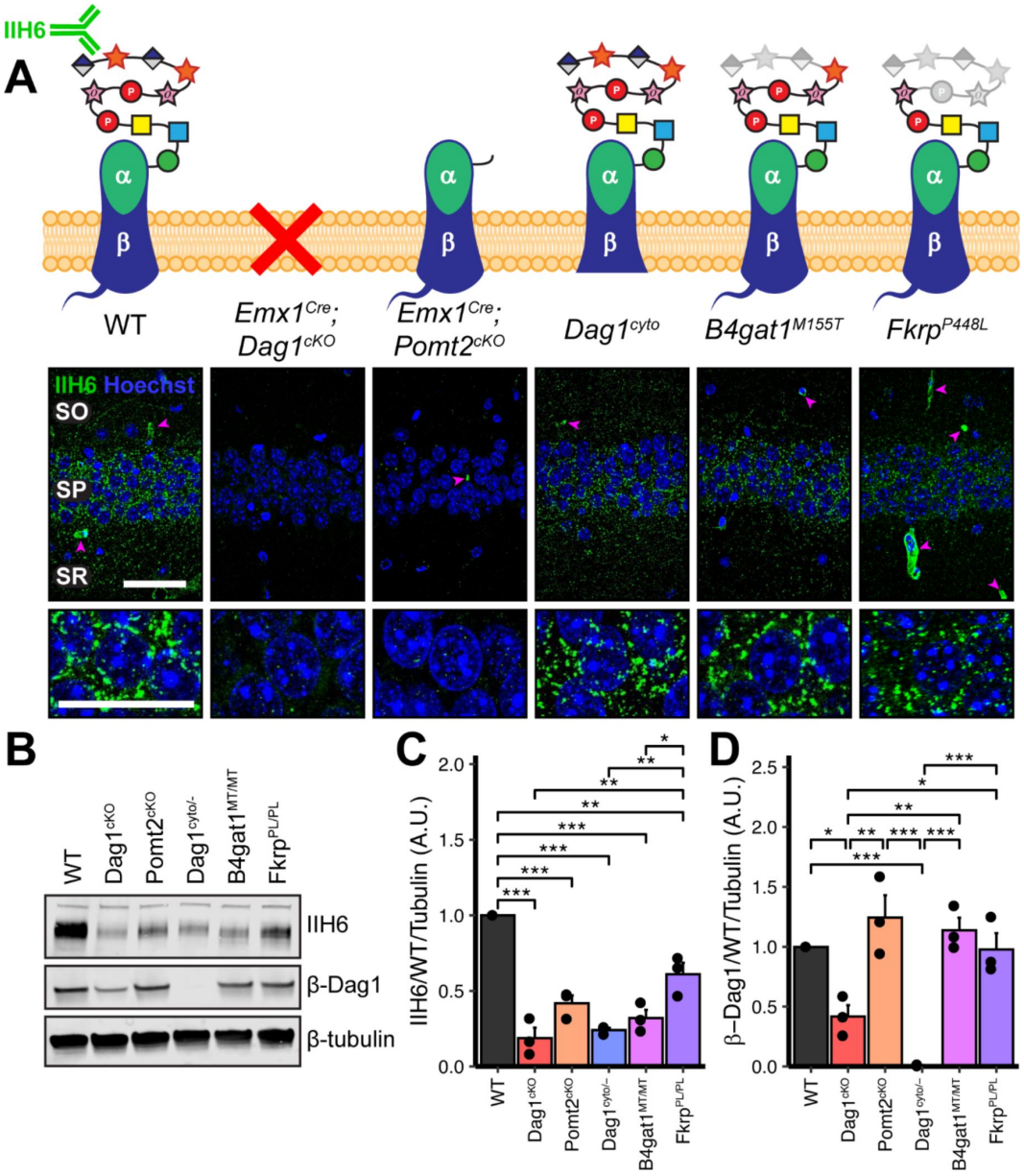

Figure 1.

Dystroglycan synaptic localization and glycosylation in mouse models of dystroglycanopathy.

(A) Schematic depiction of Dystroglycan in different mouse models. The IIH6 antibody recognizes the matriglycan repeats on extracellular αDag1. Hippocampal CA1 of P30 mice immunostained for Dystroglycan glycosylation (IIH6, green) and nuclear marker Hoechst (blue) show puncta of glycosylated Dystroglycan localized to the perisomatic region of pyramidal cells and to blood vessels (magenta arrowheads); scale bar = 50μm. Lower panels show cell bodies in SP; scale bar = 25μm. CA1 layers: SO, *stratum oriens*; SP, *stratum pyramidale*; SR, *stratum radiatum*. **(B)** WGA-enriched lysates from P0 forebrain were immunoblotted for IIH6, β-Dag1, and β-tubulin. **(C-D)** Quantification of immunoblot in **(B)**. Error bars show mean + SEM.

neurons (**Fig. 1A**). Immunoreactivity was also present in blood vessels, where *Dag1* is also expressed (Durbeej et al., 1998; Zaccaria et al., 2001). Neuronal immunoreactivity was undetectable in $Emx1^{Cre};Dag1^{cKOs}$ and $Emx1^{Cre};Pomt2^{cKOs}$, whereas blood vessel expression was maintained, illustrating the specificity of the conditional deletion (**Fig. 1A**). Punctate perisomatic IIH6 immunoreactivity was present in $Dag1^{cyto/-}$, $B4gat1^{M155T/M155T}$, and $Fkrp^{P448L/P448L}$ mice (**Fig. 1A**). To assess Dystroglycan localization in $Emx1^{Cre};Pomt2^{cKOs}$we used an antibody that recognizes the intracellular C-terminus of β-Dag1. Although immunoreactivity for β-Dag1 was present and elevated above $Emx1^{Cre};Dag1^{cKO}$or $Dag1^{cyto/-}$ levels, Dag1 localization did not appear punctate in $Emx1^{Cre};Pomt2^{cKOs}$ (**Fig. 1 Supp. 2A**). This apparent difference implies that Dag1 glycosylation, and by extension the extracellular interactions that matriglycan mediates, is required for proper Dag1 synaptic localization.

We next prepared WGA-enriched lysate from neonatal (P0) forebrain and immunoblotted for (1) IIH6, to quantify the degree of α-Dag1 glycosylation and (2) β- Dag1, to measure total Dystroglycan protein levels (**Fig. 1B**). Dag1 glycosylation was significantly reduced in $Emx1^{Cre};Dag1^{cKOs}$, $Emx1^{Cre};Pomt2^{cKOs}$, $Dag1^{cyto/-}$, $B4gat1^{M155T/M155T}$, and $Fkrp^{P448L/P448L}$ mice; however, the reduction in $Fkrp^{P448L/P448L}$ mice was less severe than the other models (**Fig. 1C**). The reduction in glycosylation observed in the $Dag1^{cyto/-}$ mice is surprising given that the mutation is restricted to the intracellular domain. *Dystroglycan* heterozygotes ($Dag1^{+/-}$) show no reduction in IIH6 levels compared to wild-types (data not shown), so the reduction in $Dag1^{cyto/-}$ mice can be presumed to be due to the intracellular deletion. It is possible that the intracellular domain is required for the trafficking of Dystroglycan through the endoplasmic reticulum and/or Golgi apparatus, where Dystroglycan undergoes glycosylation, however additional work is needed to verify this. As expected, β-Dag1 immunoblotting was significantly reduced in $Emx^{Cre};Dag1^{cKOs}$ and absent in $Dag1^{cyto/-}$ mice but normal in the glycosylation mutants (**Fig. 1D**). The residual β-Dag1 in $Emx1^{Cre};Dag1^{cKO}$ brain is likely due to *Dag1* expression in unrecombined cells, such as blood vessels, as well as unrecombined tissue that remained after the forebrain dissection.

We next examined Dag1 protein levels during synaptogenesis using WGA- enriched lysate from P21-P30 hippocampus. As expected, Dag1 glycosylation assessed by IIH6 immunoblotting was severely reduced in $Emx1^{Cre};Dag1^{cKOs}$ and $Emx1^{Cre};Pomt2^{cKOs}$but normal in $Dag1^{cyto/-}$ mice (**Fig. 1 Supp. 2B-C**). Immunoblotting for β-Dag1 showed a significant reduction in $Emx1^{Cre};Dag1^{cKOs}$and $Dag1^{cyto/-}$ mutants but normal levels in $Emx1^{Cre};Pomt2^{cKOs}$(**Fig. 1 Supp. 2B, D**). Although localization of Dag1 was not punctate in $Emx1^{Cre};Pomt2^{cKOs}$(**Fig. 1 Supp. 2A**), the overall level of β- Dag1 was normal by WGA-enrichment, which enriches for proteins in the plasma membrane (**Fig. 1 Supp. 2B, D**). It therefore remains possible that Dag1 still trafficks to the cell surface in $Emx1^{Cre};Pomt2^{cKOs}$but fails to contact presynaptic axons and therefore does not permit synaptogenesis.

Dystroglycan is required for cortical neuron migration in a glycosylation-dependent manner

In neocortex, *Dag1* expression in radial glia is required for proper migration of neurons, with *Dag1* conditional deletion from neuroepithelial cells or radial glia resulting in Type II lissencephaly (S. A. Moore et al., 2002; Pawlisz & Feng, 2011; Satz et al., 2008, 2010). This requires proper Dystroglycan glycosylation, but not its expression in neurons (Chan et al., 2010; Holzfeind et al., 2002; Hu et al., 2011; Wright et al., 2012). To compare cortical migration across our five models of dystroglycanopathy, we performed immunostaining for the upper layer marker Cux1 (layers II/III-IV) and the deep layer marker Tbr1 (layers III, VI) in P30 somatosensory cortex (**Fig. 2A-B**). $Emx1^{Cre};Dag1^{cKOs}$ and $Emx1^{Cre};Pomt2^{cKOs}$showed complete cortical dyslamination with 100% penetrance, whereas the cytoplasmic ($Dag1^{cyto/-}$) deletion mutants appeared normal (**Fig. 2C-D**). $B4gat1^{M155T/M155T}$ missense mutants showed a migration phenotype only at the cortical midline, while $Fkrp^{P448L/P448L}$ missense mutants did not show any cortical migration phenotype (**Fig. 2 C-D**, **Fig. 2 Supp. 1A**). These results indicate that cortical

migration depends on Dystroglycan glycosylation but does not require its cytoplasmic domain. Furthermore, taken with the data in **Fig. 1B-D**, they illustrate that the severity of the cortical migration phenotype scales with the degree of Dystroglycan hypoglycosylation; $Emx1^{Cre};Dag1^{cKOs}$ and $Emx1^{Cre};Pomt2^{cKOs}$ model a severe form of dystroglycanopathy (Walker-Warburg Syndrome, Muscle-Eye-Brain disease) and $B4gat1^{M155T/M155T}$ and $Fkrp^{P448L/P448L}$ mutants modeling a milder form of the disease.

To further assess the impact of our functional domain mutations, we assessed Laminin localization, the canonical interacting partner of Dystroglycan in the extracellular matrix (ECM), in adult neocortex (Ibraghimov-Beskrovnaya et al., 1992). Under WT conditions, Laminin immunoreactivity was evident at the pial surface where Laminin and Dystroglycan interact at the interface between radial glial endfeet and the cortical basement membrane (Satz et al., 2010). Laminin was also present in blood vessels, where Dystroglycan-expressing perivascular astrocytes contribute to the maintenance of water homeostasis (Menezes et al., 2014). In $Emx1^{Cre};Dag1^{cKO}$ cortex, Laminin immunoreactivity at the pial surface was patchy and vascular Laminin showed evidence of the neuronal migration phenotype described in **Fig. 2** (**Fig. 2 Supp. 2A**). Laminin immunoreactivity in $Emx1^{Cre};Pomt2^{cKO}$ cortex similarly showed a patchy appearance, albeit less severe than $Emx1^{Cre};Dag1^{cKOs}$, along with the evident cortical migration phenotype (**Fig. 2 Supp. 2B**). $Dag1^{cyto/-}$ mutants, on the other hand, exhibited normal Laminin immunoreactivity both at the pial surface and with regards to vascular organization (**Fig. 2 Supp. 2C**).

Perisomatic $CCK^+/CB1R^+$ interneuron targeting requires Dystroglycan in a non-cell autonomous manner

$CCK^+/CB1R^+$ IN innervation is largely absent from the cortex and hippocampus when *Dag1* is deleted selectively from pyramidal neurons using NEX^{Cre} (Früh et al., 2016; Miller & Wright, 2021). However, the development and function of $CCK^+/CB1R^+$ INs has not been examined in mouse models that more broadly lack *Dag1* throughout the central nervous system (CNS) and thus more accurately reflect the neuropathology of dystroglycanopathy. We focused our analysis on region CA1 of the hippocampus, as its overall architecture is grossly unaffected in each of our mouse models. Both $Emx1^{Cre};Dag1^{cKO}$ and $Emx1^{Cre};Pomt2^{cKO}$ mice exhibited a mild granule cell migration phenotype in dentate gyrus (**Fig. 3A**, yellow arrows), however CA1-CA3 showed normal pyramidal neuron organization.

In WT control mice, $CCK^+/CB1R^+$ IN axon terminals were abundant throughout the hippocampus, with their highest innervation density in the CA1 pyramidal cell body layer (*stratum pyramidale*, SP) where they form characteristic basket synapses onto pyramidal neurons (**Fig. 3A-C**, **Fig. 3 Supp. 1A**). In $Emx1^{Cre};Dag1^{cKO}$ mice, $CCK^+/CB1R^+$ axons were present but failed to target the pyramidal cell layer (**Fig. 3A-C**, **Fig. 3 Supp. 1A**), a surprising difference from the phenotype observed in $NEX^{Cre};Dag1^{cKO}$ mice which lack $CCK^+/CB1R^+$ IN innervation entirely (Früh et al., 2016; Miller & Wright, 2021) (**Fig. 3 Supp. 1C**). To confirm the $CCK^+/CB1R^+$ IN innervation pattern in the context of widespread *Dag1* deletion, we generated $Nestin^{Cre};Dag1^{cKO}$ mice. $Nestin^{Cre}$, similar to $Emx1^{Cre}$, drives *Cre* recombination in forebrain progenitors, however $Emx1^{Cre}$ recombination begins around E10.5 and $Nestin^{Cre}$ recombination begins around E11.5 (Liang et al., 2012; Tronche et al., 1999). $Nestin^{Cre};Dag1^{cKOs}$ showed the same $CCK^+/CB1R^+$ axon targeting phenotype as $Emx1^{Cre};Dag1^{cKOs}$ (**Fig. 3 Supp. 1B**), further suggesting that the observed $Emx1^{Cre};Dag1^{cKO}$ phenotype faithfully models dystroglycanopathy neuropathology.

It was previously reported that the lack of $CCK^+/CB1R^+$ IN innervation of CA1 pyramidal neurons observed in $NEX^{Cre};Dag1^{cKOs}$ was accompanied by reduced numbers of $CCK^+/CB1R^+$ INs (Miller & Wright, 2021). We therefore sought to quantify $CCK^+/CB1R^+$ IN cell density in $Emx1^{Cre};Dag1^{cKOs}$ using both NECAB1 and NECAB2 antibodies (Miczán et al., 2021). As NECAB1 is expressed by both $CCK^+/CB1R^+$ INs and PV^+ INs, we performed immunolabeling for both NECAB1 and PV and quantified the density of $NECAB1^+;PV^-$ cell bodies in CA1, finding no difference between

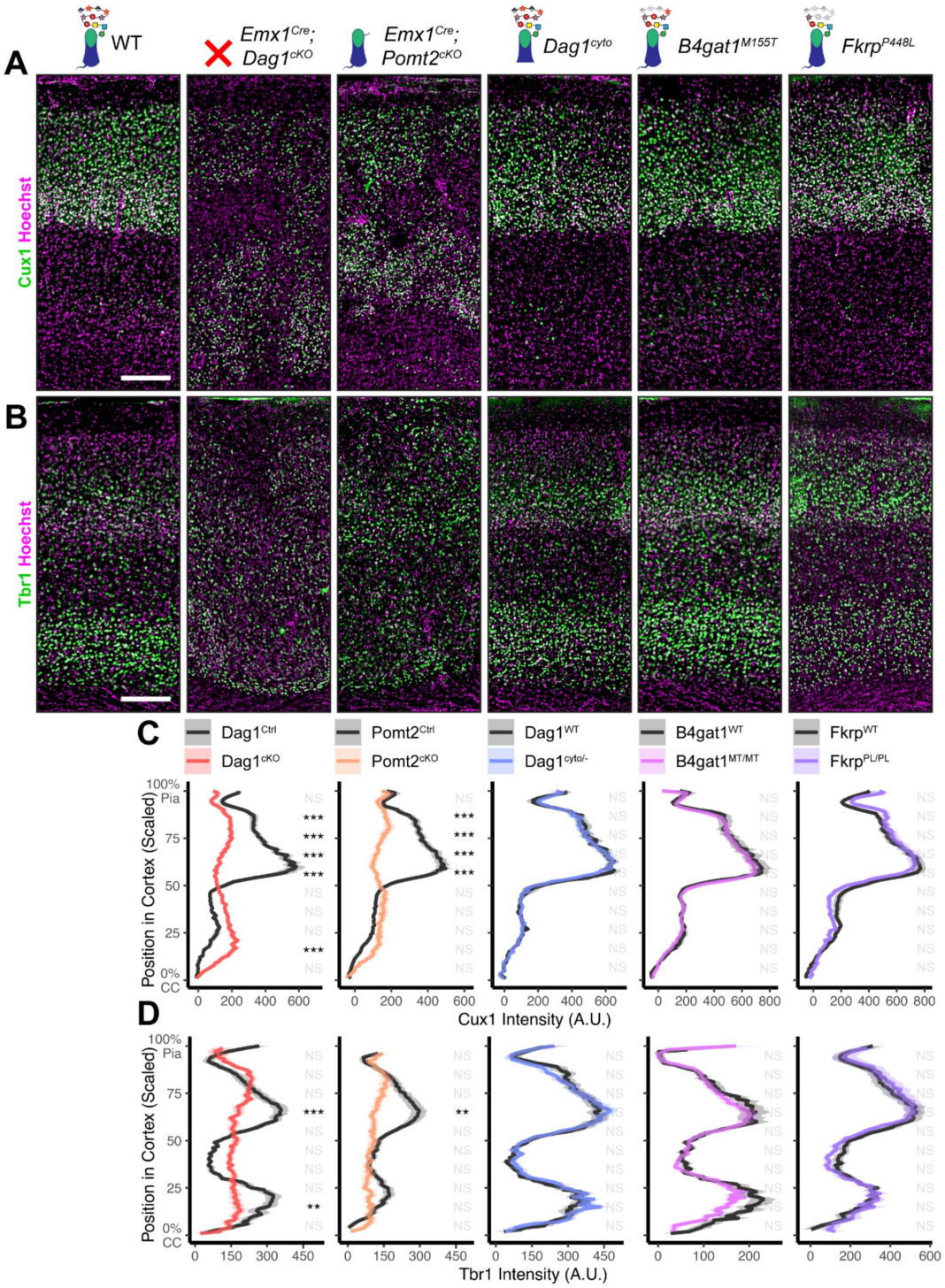

Figure 2.

Dystroglycan is required for cortical neuron migration in a glycosylation-dependent manner and independent of intracellular interactions.

Immunostaining for cortical layer markers **(A)** Cux1 (layers 2-4) and **(B)** Tbr1 (layers 3 and 6) in P30 somatosensory cortex (scale bar = 200μm). Layer markers are shown in green. Nuclear marker Hoechst is shown in magenta. Quantification of fluorescence intensity of layer markers shown for **(C)** Cux1 and **(D)** Tbr1. Shaded regions of intensity profile illustrate ± SEM. See **Supplementary Table 1** for Ns. *Significance: * = p < 0.05, ** = p < 0.01, *** = p < 0.001, NS = p ≥ 0.05. Abbreviations: CC, corpus callosum; A.U., arbitrary units*.

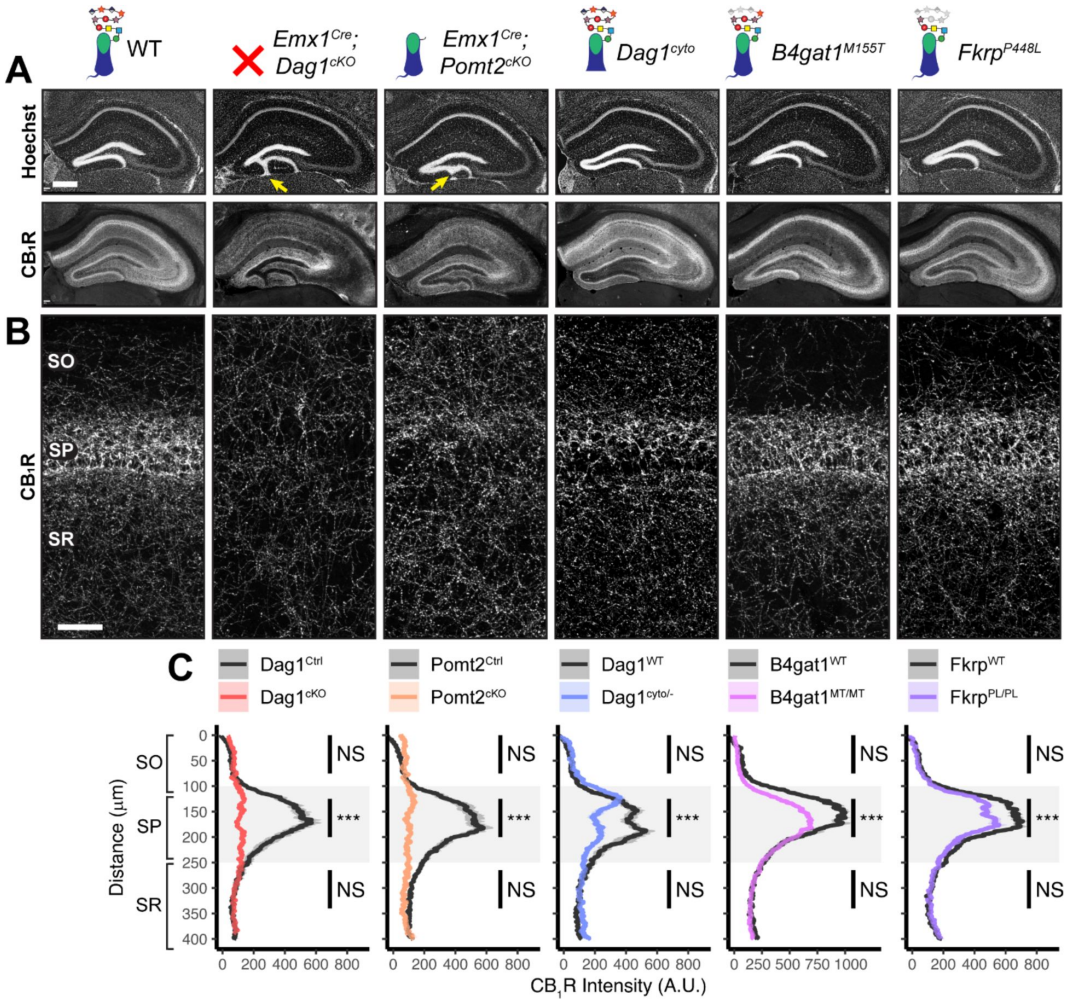

Figure 3.

Dag1 is required for CCK$^+$/CB1R$^+$ basket IN perisomatic axon targeting in *stratum pyramidale* of hippocampal CA1-3.

(A) Nuclear marker Hoechst (upper panels) shows hippocampal morphology. Granule cell migration is disrupted in dentate gyrus of *Emx1^{Cre};Dag1^{cKOs}* and *Emx1^{Cre};POMT2^{cKOs}*(yellow arrows). CA1-3 gross morphology is normal in all models. CB1R immunostaining (lower panels) shows abnormal CCK$^+$/CB1R$^+$ basket interneuron targeting in CA1-3 to varying degrees across models (scale bar = 400µm). **(B)** Higher magnification view of CB1R immunostaining in CA1 (scale bar = 50µm). **(C)** Quantification of CA1 CB1R fluorescence intensity profile. Shaded regions of intensity profile illustrate ± SEM. Gray region highlights SP. See **Supplementary Table 1** for Ns. *Significance: * = p < 0.05, ** = p < 0.01, *** = p < 0.001, NS = p ≥ 0.05. Abbreviations: A.U., arbitrary units; SO, stratum oriens; SP, stratum pyramidale; SR, stratum radiatum*.

$Emx1^{Cre};Dag1^{Ctrls}$ and $Emx1^{Cre};Dag1^{cKOs}$(**Fig. 3 Supp. 2A-B**). To confirm this, we also quantified the density of NECAB2$^+$ cell bodies in CA1, again finding no difference between genotypes (**Fig. 3 Supp. 2C, E**). Thus, the observed change in CCK$^+$/CB1R$^+$ IN axon targeting of CA1 pyramidal cells is not due to a reduction in cell numbers, but rather a failure to innervate the appropriate compartment.

$Emx1^{Cre};Pomt2^{cKO}$ mice fully phenocopied the aberrant $Emx1^{Cre};Dag1^{cKO}$ CB1R$^+$ immunoreactivity pattern (**Fig. 3A-C**), demonstrating that proper CCK$^+$/CB1R$^+$ IN basket axon targeting requires Dystroglycan glycosylation. Both the *B4gat1* and *Fkrp* mutants showed a normal distribution of CB1R$^+$ axon targeting to the somatodendritic compartment of CA1 neurons, but with reduced CB1R intensity in SP (**Fig. 3A-C**). The cytoplasmic domain of Dystroglycan also plays a role in the appropriate targeting of CB1R immunoreactive axons, as the distribution of axons was perturbed in the $Dag1^{cyto/-}$ mutants, though with an intermediate phenotype in which the upper portion of SP appeared normal while the lower portion of SP showed loss of selective CB1R$^+$ axon targeting (**Fig. 3A-C**).

Due to the axonal targeting defect in the CCK$^+$/CB1R$^+$ IN population, we next examined the parvalbumin (PV) population of interneurons in the hippocampus, as these cells also form perisomatic basket cell synapses on to CA1 pyramidal cells. There was no significant difference in the number of PV$^+$ INs in CA1 of $Emx1^{Cre};Dag1^{cKO}$mice and littermate controls (**Fig. 3 Supp. 2D, F**). Furthermore, the distribution of PV$^+$ IN axons showed normal targeting to SP in all mouse models (**Fig. 3 Supp. 3A-B**), indicating that the axon targeting phenotype is specific to the CCK$^+$/CB1R$^+$ IN population. Interestingly, $Emx1^{Cre};Dag1^{cKO}$mice exhibited a slight increase in PV intensity in SP, perhaps indicating that there is a degree of compensation (**Fig. 3 Supp. 3A-B**).

Notably, CB1R expression was also abnormal in brain regions outside of the hippocampus. In somatosensory cortex, CB1R immunostaining reflected the dyslamination phenotype in both the $Emx1^{Cre};Dag1^{cKO}$and $Emx1^{Cre};Pomt2^{cKO}$ mice throughout neocortex and the $B4gat1^{M155T/M155T}$ mice at midline, while it appeared normal in cortex of $Dag1^{cyto/-}$ and $Fkrp^{P448L/P448L}$mice (**Fig. 3 Supp. 4A**). CB1R staining was also reduced and disorganized in the basolateral amygdala (BLA) in $Emx1^{Cre};Dag1^{cKO}$ and $Emx1^{Cre};Pomt2^{cKO}$mice (**Fig. 3 Supp. 4B**). Interestingly, CB1R immunostaining in the inner molecular layer (IML) of dentate gyrus appears normal in all mutants (**Fig. 3A**). In the IML, CB1R is present in excitatory mossy cell axons targeting dentate granule cells whereas in both cortex and amygdala CB1R expression is restricted to GABAergic interneurons (Földy et al., 2006; Katona et al., 2001; Monory et al., 2015). Therefore, glycosylated Dystroglycan instructs the development of inhibitory CB1R$^+$ interneuron populations in multiple brain regions.

Dystroglycan is required for CCK$^+$/CB1R$^+$ interneuron axon targeting during early postnatal development

During early postnatal development, CCK$^+$/CB1R$^+$ IN axons undergo a dramatic laminar rearrangement, progressing from more distal localization amongst pyramidal cell dendrites, to eventually target pyramidal neuron cell bodies in the hippocampus (Miller & Wright, 2021; Morozov et al., 2009; Morozov & Freund, 2003a, 2003b). We examined the developmental time course of CCK$^+$/CB1R$^+$ IN axon targeting in our $Emx1^{Cre};Dag1^{cKO}$mice beginning at P5, when the axons are first readily identifiable (Berghuis et al., 2007; Eggan et al., 2010; Mulder et al., 2008; Vitalis et al., 2008). At P5 in control $Emx1^{Cre};Dag1^{Ctrl}$mice, CCK$^+$/CB1R$^+$ axons were initially concentrated in the *stratum radiatum* (SR) of the hippocampus (**Fig. 4A-C**). Between P10 and P30, the CCK$^+$/CB1R$^+$ axons underwent developmental reorganization, with reduced innervation of SR coinciding with a progressive increase in innervation of SP. In contrast, overall CCK$^+$/CB1R$^+$ innervation was initially reduced in the hippocampus of mutant $Emx1^{Cre};Dag1^{cKO}$mice at P5, and these axons failed to undergo laminar reorganization as they developed (**Fig. 4A-C**). By P30, after IN synapse formation and targeting are largely complete in

control mice, the density of CCK$^+$/CB1R$^+$ axons in *Emx1^{Cre};Dag1^{cKO}* mice was uniform across all hippocampal lamina (**Fig. 4A-C**). Therefore, Dystroglycan plays a critical developmental role during the first two postnatal weeks, for the proper laminar distribution and perisomatic targeting of CCK$^+$/CB1R$^+$ IN axons in the hippocampus.

CCK$^+$/CB1R$^+$ IN synapse formation requires postsynaptic glycosylated Dystroglycan

Given the perturbed distribution of CCK$^+$/CB1R$^+$ IN axons in the hippocampus, we next wanted to determine whether the remaining CCK$^+$/CB1R$^+$ IN axons were capable of forming synapses in dystroglycanopathy models. Using VGAT as a marker of inhibitory presynaptic terminals, we saw no difference in total VGAT puncta density in SP in any of the mouse models, indicating that the total number of inhibitory synapses is normal (**Fig. 5B-D**). Immunostaining for CB1R showed a significant decrease in CB1R in SP of *Emx1^{Cre};Dag1^{cKO}*, *Emx1^{Cre};Pomt2^{cKO}*, *B4gat1$^{M155T/M155T}$*, and *Fkrp$^{P448L/P448L}$* mutants, but not *Dag1$^{cyto/-}$*mutants (**Fig. 5E**). This suggests that the difference in CB1R$^+$ axon distribution described in SP of *Dag1$^{cyto/-}$*mutants in **Fig. 3A-C** likely reflects a change in CCK$^+$/CB1R$^+$ IN axon targeting but not synapse formation, whereas *Emx1^{Cre};Dag1^{cKO}*and all three glycosylation mutants exhibit a reduction in CCK$^+$/CB1R$^+$ IN axon targeting and synapse number in SP. It should be noted that the data in **Fig. 3A-C** reflects axonal CB1R intensity across all hippocampal layers, whereas the quantification in **Fig. 5E** reflects the density of axonal swellings within SP. These data therefore suggest that there is an overall reduction in CB1R intensity in SP of *Dag1$^{cyto/-}$*mutants that does not influence the number of CB1R$^+$ axonal swellings. In contrast to CCK$^+$/CB1R$^+$ INs, the PV$^+$ population of basket interneurons showed no change in puncta density in SP in any of the models (**Fig. 5 Supp. 2A-E**; analysis of VGAT, CB1R, and PV densities in SO and SR included in **Fig. 5 Supp. 1A-B** and **Fig. 5 Supp. 3A**.)

To better approximate the extent of basket synapse formation, we quantified the co-localization between VGAT and CB1R or PV. In SP, the percent of CB1R puncta co-localized with VGAT was reduced in the same models that showed a reduction in CB1R density (*Emx1^{Cre};Dag1^{cKO}*, *Emx1^{Cre};Pomt2^{cKO}*, *B4gat1$^{M155T/M155T}$*, and *Fkrp$^{P448L/P448L}$* mutants) but not *Dag1$^{cyto/-}$*mutants (**Fig. 5C, F**), suggesting that CCK$^+$/CB1R$^+$ INs require postsynaptic glycosylated Dystroglycan in order to form synapses whereas the cytoplasmic domain is required for axon targeting but not synapse formation.

Interestingly, the percent of PV co-localized with VGAT increased in the SP of *Emx1^{Cre};Dag1^{cKOs}* and *Emx1^{Cre};Pomt2^{cKOs}*mice, with no change in any of the other models (**Fig. 5 Supp. 2C, E**; analysis of co-localization in SO and SR included in **Fig. 5 Supp. 1C**, **Fig. 5 Supp. 3B**). It is possible that the reduction in inhibitory CCK$^+$/CB1R$^+$ synapses prompts homeostatic compensation through an increase in PV$^+$ synapses. Alternatively, this may reflect competition between CCK$^+$/CB1R$^+$ and PV$^+$ INs for physical space on the perisomatic region of pyramidal cells, with the decrease in CCK$^+$/CB1R$^+$ synapses in *Emx1^{Cre};Dag1^{cKOs}* and *Emx1^{Cre};Pomt2^{cKOs}* allowing additional PV$^+$ IN synapses to form.

CCK$^+$/CB1R$^+$ interneuron basket synapse function is dependent on Dystroglycan function

Perisomatic inhibitory basket cell synapses powerfully control activity in the hippocampal circuit (Freund & Katona, 2007). Previous studies in *NEX^{Cre};Dag1^{cKO}* mice, in which CCK$^+$/CB1R$^+$ INs are absent, demonstrated reduced inhibitory synaptic function (Früh et al., 2016). In the current study, however, CCK$^+$/CB1R$^+$ INs are present but mistargeted. Thus, we wanted to determine whether with the changes in CCK$^+$/CB1R$^+$ basket synapse localization in our mouse models were associated with altered inhibitory synaptic function. CCK$^+$/CB1R$^+$ IN basket cells can be selectively activated by muscarinic receptor activation, which increases the rate of spontaneous inhibitory

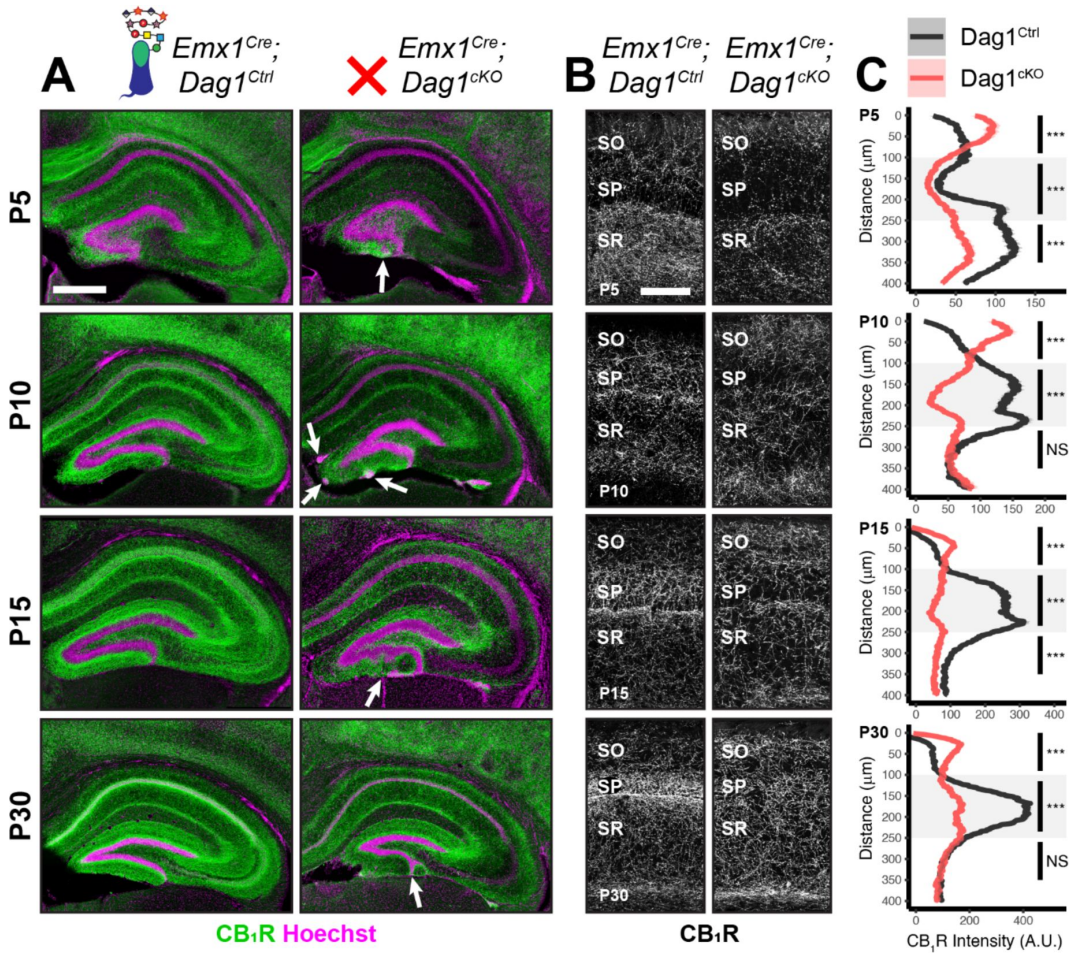

Figure 4.

Dag1 is required for CCK$^+$/CB1R$^+$ IN axon targeting during early postnatal development.

(A) Immunostaining for CB1R$^+$ axon terminals (green) in the hippocampus of *Emx1^{Cre};Dag1* controls (left) and cKOs (right) at ages P5-P30. Nuclear marker Hoechst is shown in magenta. White arrowheads indicate migration errors in dentate granule cells *Emx1^{Cre};Dag1^{cKO}*mice. Scale bar = 500µm. **(B)** Higher magnification images of CB1R$^+$ axon terminals in CA1 of *Emx1^{Cre};Dag1* controls (left) and cKOs (right) at ages P5-P30. Scale bar = 100µm. **(C)** Quantification of CB1R fluorescence intensity profile in CA1. Shaded regions of intensity profile illustrate ± SEM. Gray region highlights SP. See **Supplementary Table 1** for Ns. *Significance: * = p < 0.05, ** = p < 0.01, *** = p < 0.001, NS = p ≥ 0.05. Abbreviations: A.U., arbitrary units; SO, stratum oriens; SP, stratum pyramidale; SR, stratum radiatum*.

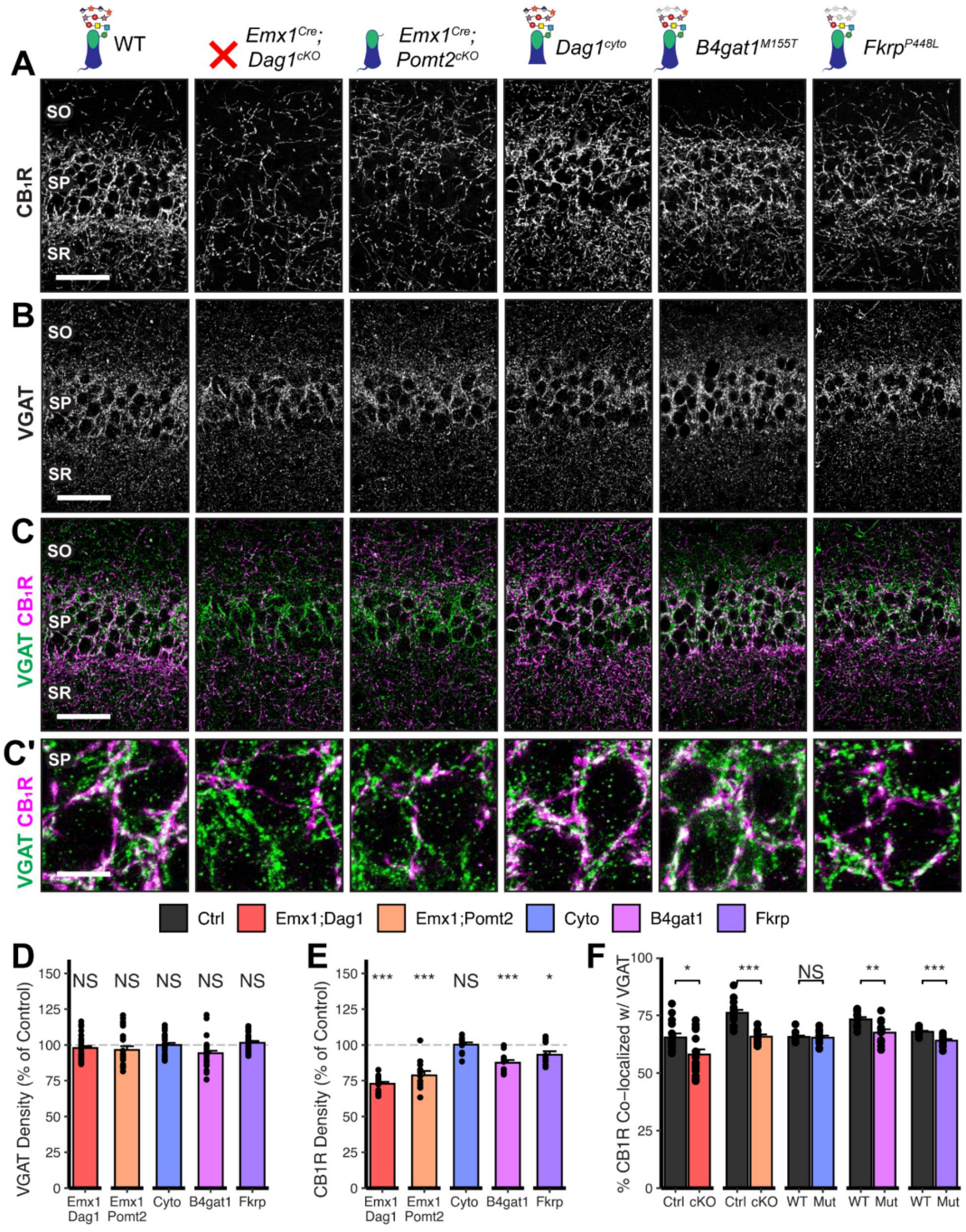

Figure 5.

Dag1 and *Pomt2* cKOs exhibit impaired CB1R$^+$ basket synapse formation in *stratum pyramidale* of hippocampal CA1.

P30 coronal sections immunostained for **(A)** CB1R and **(B)** VGAT in hippocampal CA1; merged image in **(C)** shows CB1R in magenta and VGAT in green. (A-C) Scale bar = 50µm. (Higher magnification view of SP in **(C')**; scale bar = 10µm.) **(D)** Quantification of VGAT puncta density in SP expressed as a percent of control. **(E)** Quantification of CB1R puncta density in SP expressed as a percent of control. **(F)** Quantification of co-localization between VGAT and CB1R in SP to estimate putative CB1R$^+$ basket cell synapse formation. Error bars show mean + SEM. (For quantification of puncta densities and co-localization in SO and SR see **Fig. 5 Supp. 1**.) See **Supplementary Table 1** for Ns. *Significance: * = $p < 0.05$, ** = $p < 0.01$, *** = $p < 0.001$, NS = $p \geq 0.05$. Abbreviations: SO, stratum oriens; SP, stratum pyramidale; SR, stratum radiatum*.

post-synaptic currents (sIPSCs) in nearby pyramidal cells (Früh et al., 2016; Nagode et al., 2014). Thus, to assay function at $CCK^+/CB1R^+$ IN synapses, we performed whole cell patch clamp electrophysiology from CA1 pyramidal neurons in slices from control and mutant mice. After recording 5 minutes of baseline sIPSCs, the cholinergic receptor agonist Carbachol (CCh) was added to the bath and an additional 5 minutes of sIPSCs were recorded. While both $Emx1^{Cre};Dag1^{Ctrl}$ and $Emx1^{Cre};Dag1^{cKO}$ cells displayed a CCh-mediated change in sIPSC frequency, this response was dramatically attenuated in $Emx1^{Cre};Dag1^{cKOs}$ mice compared to $Emx1^{Cre};Dag1^{Ctrl}$ mice (**Fig. 6A-C**). Furthermore, in $Emx1^{Cre};Dag1^{Ctrls}$, 19/21 cells (90.5%) responded to CCh application (defined as a >20% increase in sIPSC frequency), whereas only 13/22 cells (59.1%) responded in $Emx1^{Cre};Dag1^{cKOs}$ (**Fig. 6 Supp. 1B**). Proper Dystroglycan glycosylation was also required for $CCK^+/CB1R^+$ IN synapse function, as $Emx1^{Cre};Pomt2^{cKO}$ mice exhibited the same phenotype as $Emx1^{Cre};Dag1^{cKOs}$: a reduced response to CCh overall, and a reduced proportion of responsive cells (**Fig. 6A-C**, **Fig. 6 Supp. 1B**). CCh also increased the mean sIPSC amplitude in each of the controls (**Fig. 6 Supp. 1A**), which may reflect an increased contribution of larger-amplitude action potential-mediated perisomatic events elicited by CCh (Früh et al., 2016; Nagode et al., 2014). Consistent with the decreased function of $CCK^+/CB1R^+$ IN synapses, a CCh-mediated change in sIPSC amplitude was also absent in each of these models (**Fig. 6 Supp. 1A**). Together, these data indicate that the altered perisomatic $CCK^+/CB1R^+$ IN synaptic localization in CA1 is associated with a functional deficit in synaptic signaling.

$Dag1^{cyto/-}$ mutants also had a dramatically attenuated sIPSC response to CCh compared to WT controls (**Fig. 6C**). Notably, even baseline sIPSC frequency was reduced in $Dag1^{cyto/-}$ mutants (2.27±1.70 Hz) compared to WT controls (4.46±2.04 Hz, $p = 0.002$), whereas baseline sIPSC frequencies appeared normal in all other mutants when compared to their respective controls. Together with the finding that these mutants contain a normal number of $CCK^+/CB1R^+$ basket synapses (as measured using immunohistochemistry; **Fig. 5A-D**), these results indicate that the cytoplasmic domain of Dystroglycan may play a critical role in mediating the assembly of functional postsynaptic signaling/receptor complexes at these synapses.

Neither of the more mildly hypoglycosylated mutants ($B4gat1^{M155T/M155T}$, $Fkrp^{P448L/P448L}$) were different from their respective littermate controls in terms of the magnitude of the CCh effect on sIPSC frequency (**Fig. 6C**), although the $B4gat1^{WT}$ mice appeared to possess a reduced effect of CCh compared to other control conditions (**Fig. 6A-C**). The *B4gat1* line is of a mixed genetic background, which could possibly explain the difference in CCh response. This finding is of unclear significance and may have obscured potential differences. Importantly, however, the marked functional synaptic differences observed between the $Emx1^{Cre};Pomt2^{cKO}$, $Emx1^{Cre};Dag1^{cKO}$ and $Dag1^{cyto/-}$ mice when compared with each of their respective controls described above was not seen in either of these phenotypically milder mutants.

Together, these results suggest that Dystroglycan is required for the function of $CCK^+/CB1R^+$ IN perisomatic basket synapses in a glycosylation-dependent manner, as evidenced by the $Emx1^{Cre};Dag1^{cKO}$ and $Emx1^{Cre};Pomt2^{cKO}$ synaptic phenotypes, and that the intracellular domain of Dystroglycan is also required for normal $CCK^+/CB1R^+$ IN basket synapse function. However, we cannot rule out the possibility that $CCK^+/CB1R^+$ INs are simply less responsive to CCh in the mutants, as we lack the tools to identify $CCK^+/CB1R^+$ INs in live tissue for targeted recordings. In contrast, $B4gat1^{M155T/M155T}$ and $Fkrp^{P448L/P448L}$ hypomorphic mutants both appear to retain sufficient Dystroglycan glycosylation to maintain normal synapse function.

Increased seizure susceptibility in models of dystroglycanopathy

Human patients with dystroglycanopathy have an increased risk of seizures and epilepsy (Dhaibani et al., 2018; Di Rosa et al., 2011; Raphael et al., 2014; Yang et al., 2022), however the underlying cause has yet to be determined. The observed defects in inhibitory basket synapse function suggest that alterations in neuronal circuit inhibition could potentially

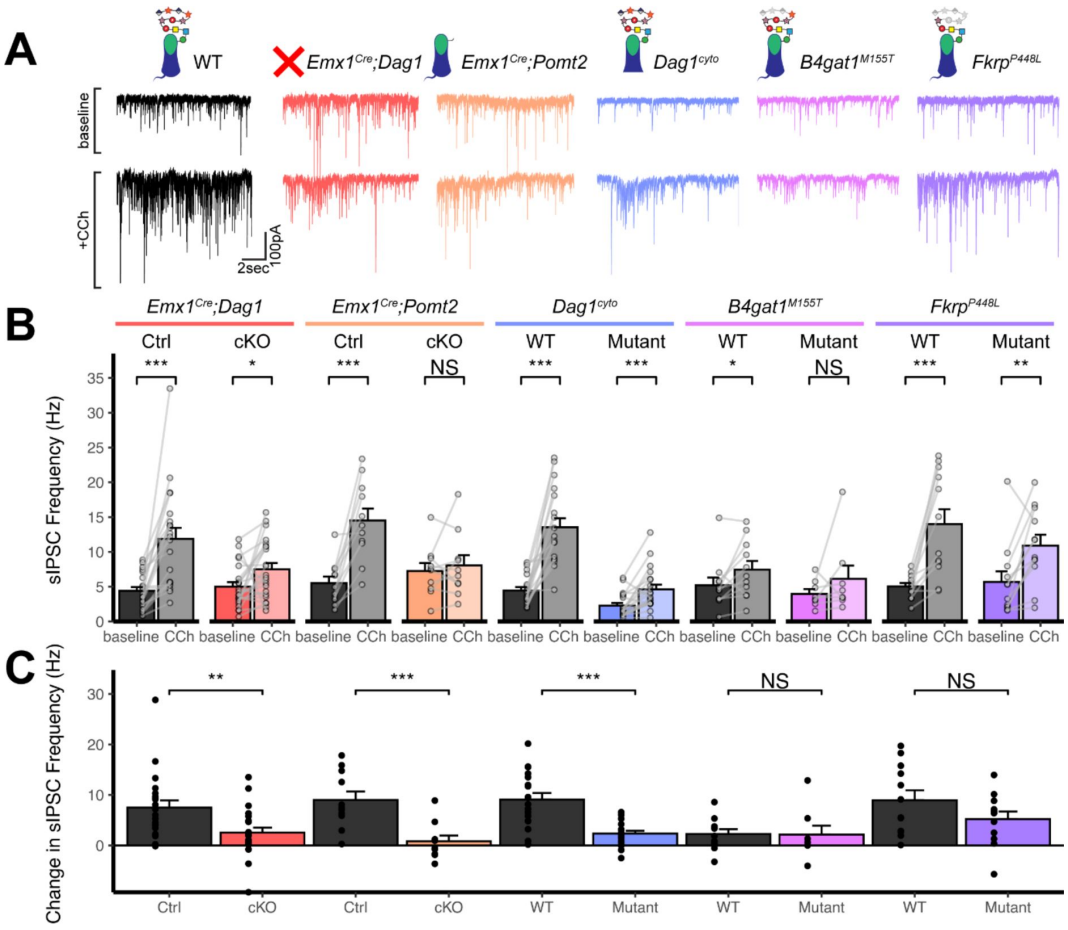

Figure 6.

Dag1 is required for CCK$^+$/CB1R$^+$ IN synapse function in hippocampal CA1 in a manner dependent on both glycosylation and intracellular interactions.

(A) Representative traces showing 15 seconds of sIPSC recordings at baseline (top) and after the addition of carbachol (bottom). **(B)** Quantification of average sIPSC frequency at baseline and after the addition of carbachol. **(C)** Quantification of the change in sIPSC frequency with the addition of carbachol. Error bars show mean + SEM. See Supplementary Table 1 for Ns. *Significance: * = $p < 0.05$, ** = $p < 0.01$, *** = $p < 0.001$, NS = $p \geq 0.05$. Abbreviations: sIPSC, spontaneous inhibitory postsynaptic current; CCh, carbachol*.

predispose mutant mice to seizures. To test whether mouse models of dystroglycanopathy exhibit a reduced seizure threshold, we exposed mice to the volatile chemoconvulsant flurothyl and measured the latency to generalized tonic-clonic seizure (TCS) (Egawa et al., 2021).

The latency to TCS was significantly faster in $Emx1^{Cre};Dag1^{cKO}$ mice than their littermate controls (a 40.9% reduction on average, **Fig. 7A**), with no difference in seizure latency between sexes in either group (**Fig. 7 Supp. 1C**). $Emx1^{Cre};Pomt2^{cKOs}$and $Dag1^{cyto/-}$ mutants also had a significantly shorter latency to TCS than littermate controls (42.9% and 33.6% reductions, respectively; **Fig. 7A**), indicating that the mechanism underlying Dystroglycan's role in seizure susceptibility requires both extracellular glycosylation and intracellular interactions. $B4gat1^{M155T/M155T}$ mutants showed a small but significant reduction (16%) in seizure latency, despite exhibiting no detectable functional deficit by electrophysiology (**Fig. 6A-C**, **Fig. 7A**). Finally, $Fkrp^{P448L/P448L}$ mutants showed no significant change in seizure susceptibility (**Fig. 7A**). Thus, the reduction in seizure latency reflects the severity of the synaptic phenotypes across the various models of dystroglycanopathy. These results demonstrate that disruptions in Dystroglycan function, including both its extracellular glycosylation and intracellular interactions, increase sensitivity to seizures.

Discussion

Recent work identified a key role for neuronal Dystroglycan in the establishment and function of $CCK^+/CB1R^+$ inhibitory synapses in the forebrain (Früh et al., 2016; Miller & Wright, 2021). Deletion of *Dag1* selectively from pyramidal neurons ($NEX^{Cre};Dag1^{cKO}$) led to a near complete loss of $CCK^+/CB1R^+$ INs during the first few postnatal weeks. In this study, we sought to better understand how $CCK^+/CB1R^+$ IN synapse formation is affected in mouse models that more accurately reflect dystroglycanopathy, in which Dystroglycan function is more broadly affected throughout the CNS (**Figs. 1**, **2**). Using a model that deletes *Dag1* throughout the developing forebrain ($Emx1^{Cre};Dag1^{cKO}$) we found that $CCK^+/CB1R^+$ INs were present, but the laminar organization of their axon terminals and their ability to form functional basket synapses onto pyramidal neuron cell bodies in the hippocampus was impaired (**Figs. 3**-**6**). The inability of $CCK^+/CB1R^+$axon terminals to concentrate in the CA1-3 cell body layer began to manifest during the first postnatal week, when dynamic changes in laminar innervation by $CCK^+/CB1R^+$ axons normally occur (**Fig. 4**). Furthermore, these mice were found to exhibit a reduced seizure threshold compared to controls, showing for the first time that mouse models of dystroglycanopathy are vulnerable to seizures (**Fig. 7**). Because $Emx1^{Cre}$(and $Nestin^{Cre}$) conditional deletion of *Dag1* or *Pomt2* leads to widespread loss of functional Dystroglycan in the forebrain in contrast with the previously studied NEX^{Cre} conditional deletion, which targets pyramidal neurons, these models more accurately model dystroglycanopathy.

We found that $CCK^+/CB1R^+$ IN synapse formation and function are dependent on proper Dystroglycan glycosylation and appear to correlate with the degree of hypoglycosylation in different mutants. Complete reduction of glycosylation in $Emx1^{Cre};Pomt2^{cKO}$mutants caused the same phenotypes seen in Dystroglycan conditional knockouts ($Emx1^{Cre};Dag1^{cKO}$) (**Figs. 1**-**3**, **5**-**6**), possibly due to the mislocalization of Dystroglycan. The finding that glycosylation is required for Dystroglycan synaptic localization in hippocampal pyramidal cells is similar to a previous finding in retinal photoreceptors in the context of *Pomt1* conditional deletion (Rubio-Fernández et al., 2018). In contrast, when *Fktn* deletion is induced in myotubes β-Dystroglycan localization is unchanged, suggesting that this phenomenon is unique to synaptic Dystroglycan (Beedle et al., 2012). One interpretation is that without matriglycan present to mediate interaction with presynaptic cells, Dystroglycan is no longer concentrated at synaptic sites, implicating it as a synaptic organizer. However, the miswiring of the $CCK^+/CB1R^+$ axons could also reduce the likelihood of postsynaptic Dystroglycan encountering a presynaptic axon, discouraging

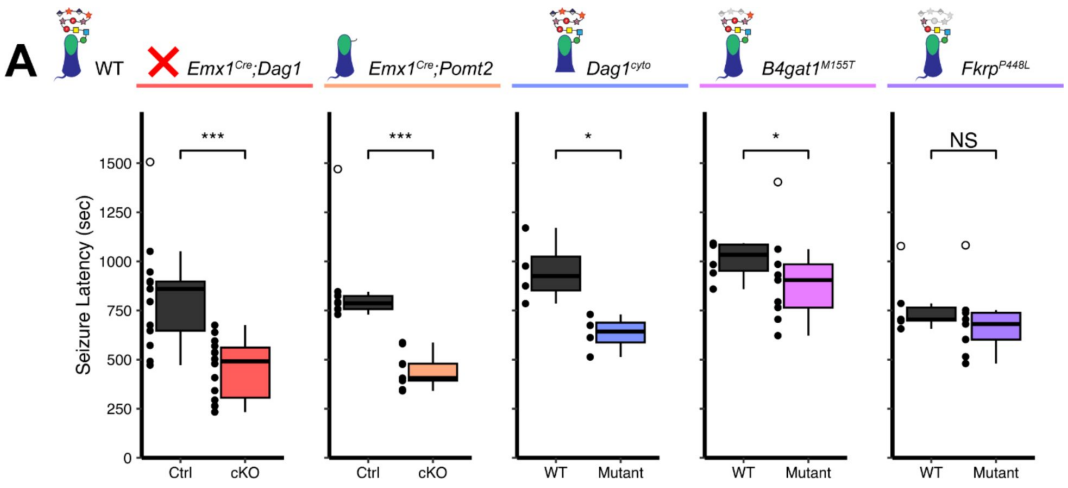

Figure 7.

Reduced seizure induction threshold in models of dystroglycanopathy.

(A) Quantification of latency (in seconds) to generalized tonic clonic seizure upon exposure to 10% flurothyl delivered at a constant rate. Open points denote statistical outliers. See **Supplementary Table 1 for Ns.** ***Significance:* * = *p* < *0.05*, ** = *p* < *0.01*, *** = *p* < *0.001*, *NS* = *p* ≥ *0.05*.**

synaptic localization. Conversely, it is possible that glycosylation is required for trafficking to the surface in the first place, however this is less likely given that the levels of β-Dystroglycan were normal in membrane-enriched lysate (**Fig. 1**, **Fig. 1 Supp. 2**).

A milder reduction in glycosylation (*B4gat1*$^{M155T/M155T}$) resulted in a cortical migration phenotype that was restricted to midline (**Fig. 3 Supp. 4**) and a small reduction in CCK^{+}/CB1R^{+} axon terminals and synaptic puncta density in CA1 which did not appear to affect synapse function (**Figs. 3**, **5**-**6**). The mildest reduction in glycosylation amongst our models was observed in *Fkrp*$^{P448L/P448L}$ mutants, which exhibited normal cortical migration but the same mild defect in CCK^{+}/CB1R^{+} IN axon targeting and synaptic puncta density observed in *B4gat1*$^{M155T/M155T}$ mutants (**Figs. 3**, **5**-**6**). Together, these three glycosylation mutants illustrate the degree of hypoglycosylation required for neurodevelopmental processes and show that defects in synaptic function only arise in the context of severely reduced glycosylation; the residual Dystroglycan function present in *B4gat1*$^{M155T/M155T}$and *Fkrp*$^{P448L/P448L}$ mutants is sufficient for most aspects of brain development. Finally, using *Dag1*$^{cyto/-}$ mutants that lack the intracellular domain of Dystroglycan, we found that the intracellular domain plays a role in some, but not all, neurodevelopmental processes. The intracellular domain is not required for neuronal migration in neocortex or synapse formation in CA1 (**Figs. 2** **and 5**) but is required for the proper targeting of CCK^{+}/CB1R^{+} IN axons in CA1- 3 (**Fig. 3**) and for subsequent CCK^{+}/CB1R^{+} IN basket synapse function (**Fig. 6**).

Dystroglycan is an essential transsynaptic organizing molecule for CCK^{+}/CB1R^{+}basket synapses

Synaptogenesis requires multiple distinct steps: (1) synaptic partner recognition, (2) recruitment and assembly of core pre- and post-synaptic machinery, (3) differentiation and maturation of synaptic identity, and (4) synaptic maintenance (Südhof, 2018). Based on data from this study (**Fig. 4**) and previous work from our group and others, mice lacking *Dystroglycan* exhibit defects in CCK^{+}/CB1R^{+} IN development at the earliest time point they can be reliably identified (P0-P5), before the peak phase of inhibitory synapse formation (P9), suggesting that Dystroglycan functions at the earliest stages of synaptogenesis such as synaptic partner recognition (Favuzzi et al., 2019). Determining the precise onset of synapse targeting and formation for most IN subtypes, including CCK^{+}/CB1R^{+}INs, is limited by a lack of genetic tools for visualizing and manipulating IN subtypes during developmental stages.

The impairment in CCK^{+}/CB1R^{+} IN development throughout the forebrain suggests a trans-synaptic role for Dystroglycan **(Fig. 3**, **Fig. 3 Supp. 4**). The identity of the trans-synaptic binding partner between Dystroglycan-expressing cells and CCK^{+}/CB1R^{+} INs remains unknown. Our data in *Emx1*^{Cre};*Pomt2*^{cKO}mice point to a critical role for the glycan chains on Dystroglycan mediating this binding. All proteins that bind to the glycan chains on Dystroglycan do so through at least one Laminin G (LG) domain. There are over 25 LG-domain containing extracellular or transmembrane proteins expressed in the hippocampus. Neurexins, a family of highly alternatively spliced synaptic cell-adhesion molecules (*NRXN1-3*) which each contain multiple LG domains, bind Dystroglycan in a glycosylation-dependent manner (Boucard et al., 2005; Fuccillo et al., 2015; Reissner et al., 2014; Sugita et al., 2001). The specific splice isoforms of *Nrxns* that bind Dystroglycan are expressed by CCK^{+}/CB1R^{+} INs (Fuccillo et al., 2015; Ullrich et al., 1995). *Neurexin-3* conditional knockout (targeting all *Nrxn3* isoforms) and CRISPR-mediated *Dag1* knockout both result in similar synaptic deficits in olfactory bulb and prefrontal cortex (Trotter et al., 2023). While a Dystroglycan knock-in mouse with reduced glycosylation that impairs Neurexin binding (*Dag1*^{T190M}) shows normal CCK^{+}/CB1R^{+} synapse formation by immunohistochemistry, the functionality of these synapses was not assessed by electrophysiology (Früh et al., 2016). Similar to *B4gat1*$^{M155T/M155T}$and *Fkrp*$^{P448L/P448L}$ mutants, the *Dag1*^{T190M} mutation does not fully eliminate Dystroglycan glycosylation, and therefore does not rule out the possibility that Neurexins play a role at CCK^{+}/CB1R^{+} synapses. It is also possible that a yet

undescribed Dystroglycan interacting protein is required for initial synapse recognition, and Nrxn-Dag1 interactions are required for subsequent synapse maturation and maintenance only. Indeed, the majority of studies indicate that Neurexins are not required for the initial formation of synapses, but rather regulate the maturation and structural maintenance of synapses after they have formed (Chen et al., 2017; Dudanova et al., 2007; Lin et al., 2023; Missler et al., 2003; Trotter et al., 2023). Interestingly, while Dystroglycan localizes to both PV^+ and $CCK^+/CB1R^+$ inhibitory basket synapses in CA1, only the $CCK^+/CB1R^+$ IN population was affected in the dystroglycanopathy models (Früh et al., 2016). Presumably, PV^+ INs have a distinct developmental program independent of Dystroglycan and likely require a different postsynaptic recognition partner.

A role for the Dystrophin-Glycoprotein Complex in $CCK^+/CB1R^+$ interneuron development

In brain and muscle tissue, Dystroglycan forms a complex with Dystrophin and several other proteins, collectively known as the Dystrophin Glycoprotein Complex (DGC). Like Dystroglycan, Dystrophin is also expressed throughout the forebrain and is associated with inhibitory synapses in multiple brain regions (Knuesel et al., 1999). Patients with mutations in *Dystrophin* develop Duchenne Muscular Dystrophy (DMD), and frequently exhibit cognitive impairments in the absence of brain malformations, suggesting a general role for the DGC in synapse development and function (Jagadha & Becker, 1988; Moizard et al., 2000; Naidoo & Anthony, 2020). A mouse model of DMD lacking all neuronal Dystrophin isoforms (*mdx*) exhibits defects in $CCK^+/CB1R^+$ IN synapse development and abnormal innervation in the hippocampus, resembling the innervation pattern we observed in $Emx1^{Cre};Dag1^{cKO}$ and $Emx1^{Cre};Pomt2^{cKO}$ mice in this study (Krasowska et al., 2014). Since Dystroglycan interacts with Dystrophin through its intracellular domain, we expected to observe similar phenotypes in mice lacking the intracellular domain of Dystroglycan ($Dag1^{cyto/-}$). However, $Dag1^{cyto/-}$ showed a milder axon targeting defect than $Emx1^{Cre};Dag1^{cKO}$ or *mdx* mice. In addition, IIH6 puncta were normally localized to the somatodendritic compartment in $Dag1^{cyto/-}$ mutants, suggesting that Dystroglycan does not require interactions with Dystrophin for is localization to somatodendritic synapses. However, Dystroglycan's synaptic localization has not been examined in the *mdx* mutants. Clearly, additional work is required to better understand the relationship between Dystroglycan and Dystrophin at synapses in the brain.

While the density of $CCK^+/CB1R^+$ IN synaptic puncta was normal in $Dag1^{cyto/-}$ mice, synaptic function was impaired to the same level as $Emx1^{Cre};Dag^{cKO}$ and $Emx1^{Cre};Pomt2^{cKO}$mice, and seizure latency was reduced. Given that $Dag1^{cyto/-}$ and $B4gat1^{M155T/M155T}$ mutants show a similar reduction in Dystroglycan glycosylation (**Fig. 1B-C**), our observation that the functional synaptic phenotype is restricted to the $Dag1^{cyto/-}$ mutant reinforces the notion that the intracellular domain of Dystroglycan plays an active role in organizing essential postsynaptic signaling elements. One possibility is that the intracellular domain of Dystroglycan is required to recruit additional postsynaptic scaffolding elements and receptors necessary for $CCK^+/CB1R^+$ basket synapse function (Uezu et al., 2019). Importantly, $Dag1^{cyto/-}$ mice did not show a cortical migration phenotype (**Fig. 2A-D**), indicating that the functional synaptic deficits and reduced seizure latency occurred independent of cortical malformation.

Altered inhibitory synapse development and function may contribute to neurological symptoms in dystroglycanopathy

In addition to muscular atrophy and hypotonia, dystroglycanopathy patients often present with central nervous system symptoms. Patients with the most severe forms of dystroglycanopathy (FCMD, Muscle-Eye-Brain disease, and Walker-Warburg Syndrome) exhibit structural changes including hypoplasia of the retina, brainstem and spinal cord, cerebellar cysts, hydrocephalus, Type II lissencephaly, and microcephaly, associated with seizures and cognitive disability (Meilleur

et al., 2014; Mercuri et al., 2009). Patients with milder forms of dystroglycanopathy may show cognitive disability and/or seizures without gross brain malformations, suggesting that there may be synaptic deficits independent of early neurodevelopmental processes (e.g. neuronal migration, axon guidance) (Mercuri et al., 2009; Yang et al., 2022). The mouse models used in this study recapitulate the full spectrum of brain malformations seen in human patients. *Emx1*^{Cre};*Dag*^{cKO}and *Emx1*^{Cre};*Pomt2*^{cKO} mice show Type II lissencephaly consistent with severe dystroglycanopathy, whereas *B4gat1*$^{M155T/M155T}$and *Fkrp*$^{P448L/P448L}$ mutants have relatively normal cortical development consistent with mild dystroglycanopathy. Mutations in any of the genes involved in the glycosylation of Dystroglycan can result in dystroglycanopathy with seizures, but the incidence and severity of seizures is higher in patients with brain malformations (Mercuri et al., 2009; Wang et al., 2017; Yang et al., 2022).

Mice have been used to model dystroglycanopathy for decades, however to our knowledge the present study is the first to investigate seizure susceptibility in mouse models of dystroglycanopathy. It is probable that the CCK^{+}/CB1R^{+} interneuron axon targeting and synapse phenotypes in the mouse models described in the present study contribute to their seizure susceptibility and open the possibility that defective inhibitory synaptic signaling mechanisms may underlie seizures in dystroglycanopathy patients. Although severe neuronal migration phenotypes In *Emx1*^{Cre};*Dag1*^{cKO}and *Emx1*^{Cre};*Pomt2*^{cKO} mice may contribute to seizure activity, our observation that *Dag1*$^{cyto/-}$mutants showed both abnormal CCK^{+}/CB1R^{+}synaptic function and reduced seizure latency, with intact cortical migration, indicates that the seizure phenotype is likely associated with synaptic defects. Supporting these results, CCK^{+}/CB1R^{+} interneurons in the hippocampus are selectively lost in models of temporal lobe epilepsy with recurrent seizures induced by pilocarpine. CCK^{+}/CB1R^{+} axons in CA1-3 begin to degenerate within hours of status epilepticus, whereas PV^{+} INs are unaffected in this model (Whitebirch et al., 2023; Wyeth et al., 2010).

While our *B4gat1*$^{M155T/M155T}$ mutants showed only a slightly reduced seizure latency, the mutants experienced more severe seizures than the other mouse models, resulting in death in 50% of cases (4/8 mutants compared to 0/6 fatalities among littermate controls) (**Fig. 7 Supp. 1A**). Flurothyl-induced seizures are typically generalized forebrain seizures; however in seizure-prone mouse models or in mice exposed to higher concentrations of flurothyl, mice can experience a suppression of brainstem oscillations followed by sudden death (Gu et al., 2022; Kadiyala et al., 2016). The *B4gat1*$^{M155T/M155T}$ mutation was originally identified based on a hindbrain axon guidance phenotype, suggesting they may have currently unknown defects in brainstem development or circuitry that could render them more susceptible to fatal brainstem seizures (Wright et al., 2012). Because the *Dag1* and *Pomt2* mutants are forebrain-specific conditional knockouts, (**Fig. 1 Supp. 1A**), we would not anticipate abnormal axon guidance in the brainstem or hindbrain of these mutants. Further research on the nature and progression of seizures observed in mouse models may have a profound impact on our understanding of dystroglycanopathy and potential therapeutic interventions.

Potential therapeutics for the restoration of synapse function in patients with dystroglycanopathy

Most patients with dystroglycanopathy present with mutations in one of the 19 genes required for the glycosylation of Dystroglycan, resulting in hypoglycosylated Dystroglycan. We have demonstrated that a mild reduction in the glycosylation of Dystroglycan, as seen in *Fkrp*$^{P448L/P448L}$ and *B4gat1*$^{M155T/M155T}$ mutants, does not significantly disrupt synapse function. This suggests that glycosylation may not need to be restored to wild-type levels in order to achieve normal synapse function. Gene replacement therapy may be well suited to treat certain forms of dystroglycanopathy by rescuing glycosylation. AAV-mediated delivery of fully functional glycosyltransferases has been shown to significantly improve muscle pathology and function in dystrophic mice, however synaptic phenotypes have not been examined (Kanagawa, 2021).

Supplementation with (CDP)-ribitol, which is synthesized by *CRPPA* (previously known as *ISPD*), can restore functional Dystroglycan glycosylation and improve muscle function in mouse models with hypomorphic mutations in *CRPPA* or *Fkrp* (Cataldi et al., 2018). In mice lacking functional *CRPPA* or *Fkrp* in skeletal muscle, (CDP)-ribitol can further enhance the therapeutic impact of gene restoration (Cataldi et al., 2020). However, whether (CDP)-ribitol treatment can improve Dystroglycan function in other models of dystroglycanopathy, or is capable of restoring Dystroglycan glycosylation and synaptic function in the nervous system, remains untested.

Conclusion

We demonstrate that Dystroglycan is critical for the postnatal development of $CCK^+/CB1R^+$ interneuron axon targeting and synapse formation/function in the hippocampus of severe mouse models of dystroglycanopathy. Extracellular glycosylation of Dystroglycan and intracellular interactions involving the cytoplasmic domain are both essential for Dystroglycan's synaptic organizing role. Mice with a partial reduction in glycosylation have relatively normal $CCK^+/CB1R^+$ interneuron axon targeting and synapse function, suggesting that even a partial restoration of glycosylation may have some therapeutic benefit. These findings suggest that $CCK^+/CB1R^+$ interneuron axon targeting defects may contribute to cognitive impairments and seizure susceptibility in dystroglycanopathy.

Materials and methods

Animal husbandry

All animals were housed and cared for by the Department of Comparative Medicine (DCM) at Oregon Health and Science University (OHSU), an AAALAC- accredited institution. Animal procedures were approved by OHSU Institutional Animal Care and Use Committee (Protocol # IS00000539), adhered to the NIH *Guide for the care and use of laboratory animals*, and provided with 24-hour veterinary care. Animal facilities are regulated for temperature and humidity and maintained on a 12-hour light-dark cycle and were provided food and water *ad libitum*. Animals older than postnatal day 6 (P6) were euthanized by administration of CO2, animals <P6 were euthanized by rapid decapitation.

Mouse strains and genotyping

The day of birth was designated postnatal day 0 (P0). Ages of mice used for each analysis are indicated in the figure and figure legends. Mouse strains used in this study have been previously described and were obtained from Jackson Labs, unless otherwise indicated (**Table 1**) (Chan et al., 2010; Cohn et al., 2002; Goebbels et al., 2006; Gorski et al., 2002; Hu et al., 2011; Peron et al., 2015; Satz et al., 2009; Tronche et al., 1999; Wright et al., 2012). Breeding schemas are as described in **Table 2**. Where possible, mice were maintained on a C57BL/6 background. $Dag1^{cyto/-}$ mice occurred at a frequency lower than Mendelian, suggesting that a proportion of progeny die embryonically. To increase viability of pups, the $Dag1^{cyto}$ line was outcrossed to a CD-1 background for one generation. The *B4gat1* line has a mixed genetic background: it was founded on a C3H/He background and then crossed on to C57BL/6 for future generations. Genomic DNA extracted from toe or tail samples (Quanta BioSciences) was used to genotype animals. Primers for genotyping can be found on the JAX webpage or originating article. For each mouse strain, littermate controls were used for comparison with mutant mice. For all experiments, unless otherwise noted, mice of both sexes were used indiscriminately. See **Supplementary Table 1** for a summary of sexes used in each experiment.

Common name	Strain name	Reference	Stock #
Dag1^{Flox}	*B6.129(Cg)-Dag1$^{tm2.1Kcam}$/J*	(Cohn et al., 2002)	009652
Dag1^{cyto}	N/A	(Satz et al., 2009)	N/A
Pomt2^{Flox}	*POMT2tm1.1Hhu/J*	(Hu et al., 2011)	017880
B4gat1^{M155T}	*B6(C3)-B4GAT1^{m1Ddg}/J*	(Wright et al., 2012)	022018
Fkrp^{P448L}	*C57BL/6NJ-Fkrp^{em1Lgmd}/J*	(Chan et al., 2010)	034659
R26$^{LSL-H2B-mCherry}$	*B6.Gt(ROSA)26Sor$^{tm1.1Ksvo}$*	(Peron et al., 2015)	023139
Emx1^{Cre}	*B6.129S2-Emx1$^{tm1(cre)Krj}$/J*	(Gorski et al., 2002)	005628
Nestin^{Cre}	*B6.Cg-Tg(Nes-cre)^{1Kln}/J*	(Tronche et al., 1999)	003771
NEX^{Cre}	*NeuroD6$^{tm1(cre)Kan}$*	(Goebbels et al., 2006)	MGI:4429523

Table 1.

Mouse strains

Breeding Scheme	Control Genotype	Mutant Genotype
$Emx1^{Cre/+};Dag1^{+/-}$ x $Dag1^{Flox/Flox}$	$Emx1^{Cre/+};Dag1^{Flox/+}$	$Emx1^{Cre/+};Dag1^{Flox/-}$
$Nestin^{Cre/+};Dag1^{+/-}$ x $Dag1^{Flox/Flox}$	$Nestin^{Cre/+};Dag1^{Flox/+}$	$Nestin^{Cre/+};Dag1^{Flox/-}$
$NEX^{Cre/+};Dag1^{+/-}$ x $Dag1^{Flox/Flox}$	$NEX^{Cre/+};Dag1^{Flox/+}$	$NEX^{Cre/+};Dag1^{Flox/-}$
$Emx1^{Cre/+};Pomt2^{Flox/+}$ x $Pomt2^{Flox/Flox}$	$Emx1^{Cre/+};Pomt2^{Flox/+}$	$Emx1^{Cre/+};Pomt2^{Flox/Flox}$
$Dag1^{cyto/+}$ x $Dag1^{+/-}$	WT	$Dag1^{cyto/-}$
$B4gat1^{M155T/+}$ x $B4gat1^{M155T/+}$	WT	$B4gat1^{M155T/M155T}$
$Fkrp^{P448L/+}$ x $Fkrp^{P448L/+}$	WT	$Fkrp^{P448L/P448L}$

Table 2.

Breeding schemes

Perfusions and tissue preparation

Brains from mice younger than P15 were dissected and drop fixed in 5 mLs of 4% paraformaldehyde (PFA) in phosphate buffered saline (PBS) overnight for 18-24 hours at 4°C. Mice P15 and older were deeply anesthetized using CO2 and transcardially perfused with ice cold 0.1M PBS for two minutes to clear blood from the brain, followed by 15 mLs of ice cold 4% PFA in PBS. After perfusion, brains were dissected and post-fixed in 4% PFA for 30 minutes at room temperature. Brains were rinsed with PBS, embedded in 4% low-melt agarose (Fisher cat. no. 16520100), and sectioned at 50µm using a vibratome (VT1200S, Leica Microsystems Inc., Buffalo Grove, IL) into 24-well plates containing 1 mL of 0.1M PBS with Sodium Azide.

Immunohistochemistry

Single and multiple immunofluorescence detection of antigens was performed as follows: free-floating vibratome sections (50µm) were briefly rinsed with PBS, then blocked for 1 hour in PBS containing 0.2% Triton-X (PBST) plus 10% normal goat or donkey serum. Sections were incubated with primary antibodies (**Table 3**) diluted in blocking solution at 4°C for 48-72 hours. For staining of Dystroglycan synaptic puncta, an antigen retrieval step was performed prior to incubation in primary antibody. Briefly, sections were incubated in sodium citrate solution for 15 min at 95 degrees in a water bath. Following incubation in primary antibody, sections were rinsed with PBS then washed with PBST three times for 20 min each. Sections were then incubated with a cocktail of secondary antibodies (1:500, Alexa Fluor 488, 546, 647) in blocking solution overnight at room temperature. Sections were washed with PBS three times for 20 min each and counterstained with Hoechst 33342 (1:10,000, Life Technologies, Cat# H3570) for 20 min to visualize nuclei. Finally, sections were mounted on slides using Fluoromount-G (SouthernBiotech) and sealed using nail polish.

Microscopy

Imaging was performed on either a Zeiss Axio Imager M2 fluorescence upright microscope equipped with an Apotome.2 module or a Zeiss LSM 980 laser scanning confocal build around a motorized Zeiss Axio Observer Z1 inverted microscope with a Piezo stage. The Axio Imager M2 uses a metal halide light source (HXP 200 C), Axiocam 506 mono camera, and 10X/0.3 NA EC Plan-Neofluar, 20X/0.8 NA Plan-Apochromat objectives. The LSM 980 confocal light path has two multi-alkali PMTs and two GaAsP PMTs for four track imaging. Confocal images were acquired using a 63X/1.4 NA Plan-Apochromat Oil DIC M27 objective. Z-stack images were acquired and analyzed offline in ImageJ/FIJI (Schindelin et al., 2012) or Imaris 9.8 (Oxford Instruments). Images used for quantification between genotypes were acquired using the same exposure times. Brightness and contrast were adjusted in FIJI to improve visibility of images for publication. Figures were composed in Adobe Illustrator 2023 (Adobe Systems).

Image Quantification

For imaging experiments, 4-8 images were acquired from 2-4 coronal sections per animal, and at least three animals per genotype were used for analysis.

Cortical Lamination

Images of somatosensory cortex were acquired using a 10X objective on a Zeiss Axio Imager M2. 4µm z-stacks covering 16µm were acquired and multiple tiles were stitched together. Maximum projections were used for analysis. In FIJI, the straight line tool with a 300µm line width was used to measure the fluorescence profile from corpus callosum to pial surface. Background fluorescence was determined as the average fluorescence of the 20 darkest pixels; background was then subtracted from all points. The cortical distance was broken into 10 bins and average fluorescence within each bin was compared between genotypes.

Target	Host	Dilution	Source	Catalog #	RRID
α-Dystroglycan (IIH6C4)	Mouse	1:250	Millipore	05-593	AB_309828
β-Dystroglycan	Mouse	1:50	Leica Biosystems	NCL-b-DG	AB_442043
CB1R	Guinea pig	1:1000	Synaptic Systems	258-104	AB_2661870
Cux1	Rabbit	1:500	Santa Cruz Biotech	sc-13024	AB_2261231
Laminin	Rabbit	1:1000	Sigma	L9393	AB_477163
NECAB1	Rabbit	1:500	Sigma	HPA023629	AB1848014
NECAB2	Rabbit	1:500	Proteintech	12257-1-AP	AB_2877841
NeuN	Mouse	1:250	Millipore	MAB377	AB_2298772
Parvalbumin	Rabbit	1:1000	Swant	PV27	AB_2631173
Parvalbumin	Mouse	1:50	Swant	235	AB_10000343
Somatostatin	Rabbit	1:2000	Peninsula Labs	T-4103	AB_518614
Tbr1	Rabbit	1:500	Millipore	AB10554	AB_10806888
VGAT	Rabbit	1:500	Synaptic Systems	131-003	AB_887869
VGAT	Guinea Pig	1:500	Synaptic Systems	131-005	AB_1106810
VGlut3	Rabbit	1:1000	Synaptic Systems	135-203	AB_887886
VIP	Rabbit	1:1000	ImmunoStar	20077	AB_572270

Table 3.

Primary antibodies used for immunohistochemistry

Hippocampal CA1 CB1R and PV Distribution

Images of dorsal hippocampal CA1 were acquired using a 20X objective on a Zeiss Axio Imager M2. Maximum projection images of 0.6µm z-stacks covering 9µm were analyzed in FIJI. The straight line tool with a 300µm line width was used to measure the fluorescence profile within SO, SP, and SR of CA1, avoiding Parvalbumin$^+$ cell bodies. Background fluorescence was determined as the average fluorescence of the 50 darkest pixels; background was then subtracted from all points. The thickness of SP was determined using Hoechst fluorescence. Average fluorescence within SO/SP/SR was compared between genotypes.

Interneuron Cell Counts in CA1

Images of dorsal hippocampal CA1 were acquired using a 10X objective on a Zeiss Axio Imager M2. Maximum projection images of 4µm z-stacks covering 40µm were analyzed in FIJI. Immunolabeled NECAB1/NECAB2/PV cell bodies were counted if they were within 100µm of *stratum pyramidale*. The freehand line tool was used to measure the length of *stratum pyramidale*. Cell number was normalized to the length of *stratum pyramidale* present in the analyzed region.

Hippocampal CB1R/PV/VGAT Density and Co-localization

Images of dorsal hippocampal CA1 were acquired using a 63X objective on a Zeiss LSM 980. 0.2µm z-stacks covering 3µm were analyzed in Imaris. Hoechst fluorescence was used to determine the bounds of SP. The Imaris Spots function was used to determine the location of synaptic puncta in 3-dimensional space. Synaptic puncta were deemed to be co-localized if they were within 1µm of each other.

Western Blot

Cortex or hippocampus was dissected and solubilized in 1 mL of lysis buffer containing 100mM NaCl, 50nM Tris, 2.5mM CaCl2, 1% Triton X-100, 1% n-Octyl-β-D- glucopyranoside, and protease inhibitors. Lysate was incubated at 4°C for 1 hour and then spun at 12,500g for 25 minutes. Supernatant containing 3,000µg (cortex) or 2,000µg (hippocampus) of protein (as determined by Pierce BCA Protein Assay) was applied to agarose-bound Wheat Germ Agglutinin (WGA) (Vector Labs) overnight at 4°C. Beads were washed 3X in TBS and boiled in 1X LDS sample buffer with 2-Mercaptoethanol (1:100) for 5 minutes. Samples were run on a 4-15% gradient polyacrylamide gel at 100V for 75 minutes and then transferred to a PVDF membrane (100V for 100 minutes). For immunoblotting, membranes were blocked in 5% milk TBST and then incubated overnight at 4°C in 5% milk TBST containing primary antibody.

Antibodies used: α-Dystroglycan (IIH6C4) (Millipore cat. no. 05-593, mouse IgM, 1:500), MANDAG2 (DSHB cat. no. 7D11, mouse IgG1, 1:500), β3-tubulin (Cell Signaling Technology cat. no. 5568, rabbit, 1:2000). Membranes were washed 3X in TBST and incubated on fluorescent IRDye secondary antibody (1:10,000, LI-COR) in 5% milk TBST for 1 hour at room temperature. Membranes were imaged using a LI-COR Odyssey CLx 0918 imager and signal analyzed using LI-COR Image Studio Lite version 5.2.

Electrophysiology

For acute slice preparation, mice were deeply anesthetized in 4% isoflurane and subsequently injected with a lethal dose of 2% 2, 2, 2-Tribromoethanol in sterile water followed by transcardial perfusion with 10 mL ice cold cutting solution containing the following (in mM): 93 NMDG, 2.5 KCl, 1.2 NaH2PO4, 30 NaHCO3, 20 HEPES, 24 glucose, 5 Na Ascorbate, 2 Thiourea, 3 Na Pyruvate, 13 N-Acetyl Cysteine, 1 Kynurenic acid, 10 MgSO4, 0.5 CaCl2; pH 7.3, 300-340mmol/kg. After rapid decapitation, the brain was briefly submerged in ice cold cut solution bubbled with carbogen (95% oxygen, 5% CO2) and then sectioned into 300µm sagittal sections (Leica VT1200S vibratome) in

bubbled ice-cold cut solution. Slices were recovered in 37°C cut solution, bubbled, for 15 minutes followed by 1 hour in room temperature recording ACSF (containing, in mM: 125 NaCl, 25 NaHCO3, 1.25 NaH2PO4, 3 KCl, 25 D-Glucose, 2 CaCl2, 1 MgCl2) with an osmolarity of 310-320mmol/kg and supplemented with 1.5mM Na Ascorbate, bubbled.

CA1 pyramidal cells were patched in whole cell configuration using 3-5MΩ borosilicate glass pipettes filled with high chloride internal solution containing the following (in mM): 125 CsCl, 2.5 MgCl2, 0.5 EGTA, 10 HEPES, 2 Mg-ATP, 0.3 Na-GTP, 5 QX-314; pH 7.2, 300mmol/kg. Pipettes were wrapped in parafilm to reduce capacitive currents. Cells were voltage clamped at -70mV and continuously superfused with 2-3 mL/min bubbled recording ACSF (310-320mmol/kg) containing 10μM NBQX to block excitatory transmission. Recordings were performed at 34°C. After 5 minutes of spontaneous IPSC (sIPSC) recording, 10μM Carbachol was added to the perfusate and another 5 minutes of sIPSC were recorded. Slices were discarded after exposure to Carbachol. Signals were amplified with an AxoPatch 200B amplifier (Molecular Devices), low-pass filtered at 5 kHz, and digitized and sampled at 10 kHz with a NIDAQ analog-to-digital board (National Instruments). Data were acquired and analyzed using a custom script in Igor Pro 8 (Wavemetrics). A hyperpolarizing step of -10mV was applied before each sweep to monitor input resistance, series resistance, and measure cell capacitance. Series resistance was not compensated and was maintained below 20MΩ. Cells were excluded if series resistance changed by more than 25%.

To calculate the proportion of cells that responded to Carbachol, cells were sorted into “responsive” and “non-responsive” categories. Cells were categorized as responsive if sIPSC frequency increased by 20% or more with the addition of Carbachol. If sIPSC frequency in a cell changed by less than 20% or less than 0.5Hz it was deemed non-responsive.

Flurothyl Seizure Induction

Mice aged P40-P55 were used for the flurothyl-induced seizure susceptibility assay to determine seizure threshold. Briefly, mice were placed in an enclosed glass chamber equipped with a vaporization chamber out of reach of the mouse. Volatile liquid 10% Bis (2,2,2-Trifluorotheyl) Ether (Millipore Sigma cat. no 287571) in 95% EtOH was delivered to the vaporization chamber at a rate of 6 mL/hour. Seizure latency was determined as the amount of time until generalized tonic-clonic seizure (TCS). Upon exhibiting TCS, animals were immediately removed from the chamber and returned to their home cage, whereupon seizures ceased rapidly. Sample size was determined using power analysis as described below. The *Emx1^{Cre};Dag1* experimental groups were powered sufficiently to determine sex differences. Because no sex difference was found (**Fig. 7 Supp. 1C**), sexes were pooled for the remaining experiments. For statistical tests, outliers were excluded. Outliers were calculated as follows: first, the interquartile range (IQR) was calculated and multiplied by 1.5. This 1.5*IQR value was subtracted from the 25% quartile (Q1) and added to the 75% quartile (Q3). Points outside of the range Q1 - 1.5*IQR < x < Q3 + 1.5*IQR were categorized as outliers and indicated as such on all graphs. This was done to remove bias from extreme outliers observed in this experiment.

Statistical analysis

Phenotypic analyses were conducted using tissue collected from at least three mice per genotype from at least two independent litters. The number of mice and replicates used for each analysis (“N”) are indicated in **Supplementary Table 1**. Power analysis using pilot data was used to determine samples sizes with α = 0.05 and β = 0.80. Phenotypes were indistinguishable between male and female mice and were analyzed together. In many cases, highly penetrant phenotypes revealed the genotypes of the mice and no blinding could be performed. For comparisons between two groups, significance was determined using a two-tailed Students t-test. For comparisons between more than two groups, significance was determined using a 2-way ANOVA with Tukey HSD post-hoc analysis. Statistical significance was set at α = 0.05 ($p < 0.05$) and data presented as means ± SEM. Statistical analyses and data visualization were performed in R (version 4.0.2).

Data availability

The data that support the findings of this study are available from the corresponding author upon reasonable request.

Acknowledgements

This work was funded by NIH Grants R01NS091027 (KMW), R01NS126247 (ES) CureCMD (KMW), F31NS120649 (JNJ), F31NS108522 (DSM), P30NS061800 (OHSU ALM), VA I01-BX004938 (ES), Department of Defense W81XWH-18-1-0598 (ES). The contents of this manuscript do not represent the views of the US Department of Veterans Affairs or the US government.

Competing interests

The authors declare that they have no competing interests.

Author Contributions

J.N.J., D.S.M, E.S., and K.M.W. designed experiments. J.N.J, D.S.M., and M.K. performed experiments. J.N.J and D.S.M performed data analysis. J.N.J, D.S.M., and K.M.W. wrote the manuscript.

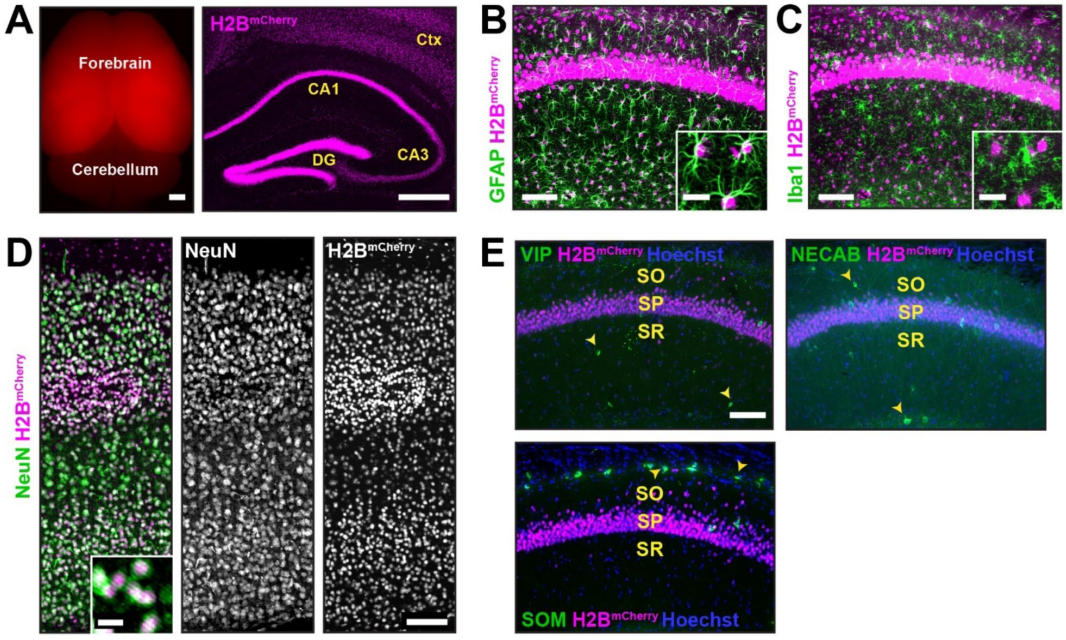

Figure 1 Supplement 1.

Emx1^{Cre} drives recombination in forebrain excitatory neurons and astrocytes, but not interneurons or microglia.

(A) Left; endogenous red fluorescence in the forebrain of P60 *Emx1*^{Cre};*R26*$^{LSL\text{-}H2B\text{-}mCherry}$ reporter mice (scale bar = 1mm). Right; coronal section of the forebrain from *Emx1*^{Cre};*R26*$^{LSL\text{-}H2B\text{-}mCherry}$ mice showing robust nuclear mCherry signal (magenta) in the cortex and hippocampus (scale bar = 500μm). **(B-E)** mCherry^{+} nuclei shown with markers of multiple cell types in the brain including astrocytes (GFAP, green) **(B)**, microglia (Iba1, green) **(C)**, and neurons (NeuN, green) **(D)** (scale bar = 100μm). Insets show enlarged images of mCherry^{+} nuclei with cell type markers (scale bar = 20μm). **(E)** mCherry^{+} nuclei with markers for different interneuron subtype markers (yellow arrowheads) (scale bar = 100μm) (VIP = Vasoactive intestinal peptide, NECAB = Neuronal calcium-binding protein 1, SOM = Somatostatin). *CA1 layers: SO, stratum oriens; SP, stratum pyramidale; SR, stratum radiatum*.

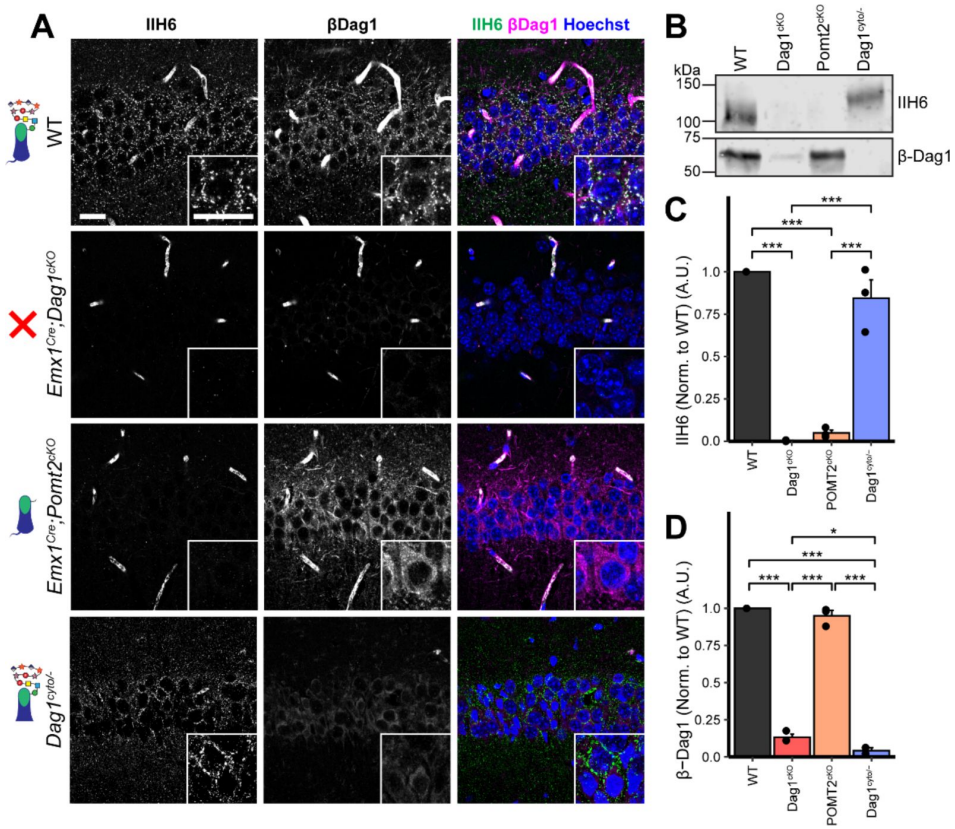

Figure 1 Supplement 2.

Dystroglycan glycosylation is required for synaptic localization.

(A) Immunostaining for matriglycan (IIH6, green) and β-Dag1 (magenta) in CA1 pyramidal cells of WT controls, *Emx1*^{Cre}*;Dag1*^{cKOs}, *Emx1*^{Cre}*;Pomt2*^{cKOs}, and *Dag1*$^{cyto/-}$ mutants. Scale bars = 25μm. **(B)** WGA-enriched lysates from P21-P30 hippocampus were immunoblotted for IIH6 and β-Dag1. **(C-D)** Quantification of immunoblot in **(B)**. Error bars show mean + SEM.

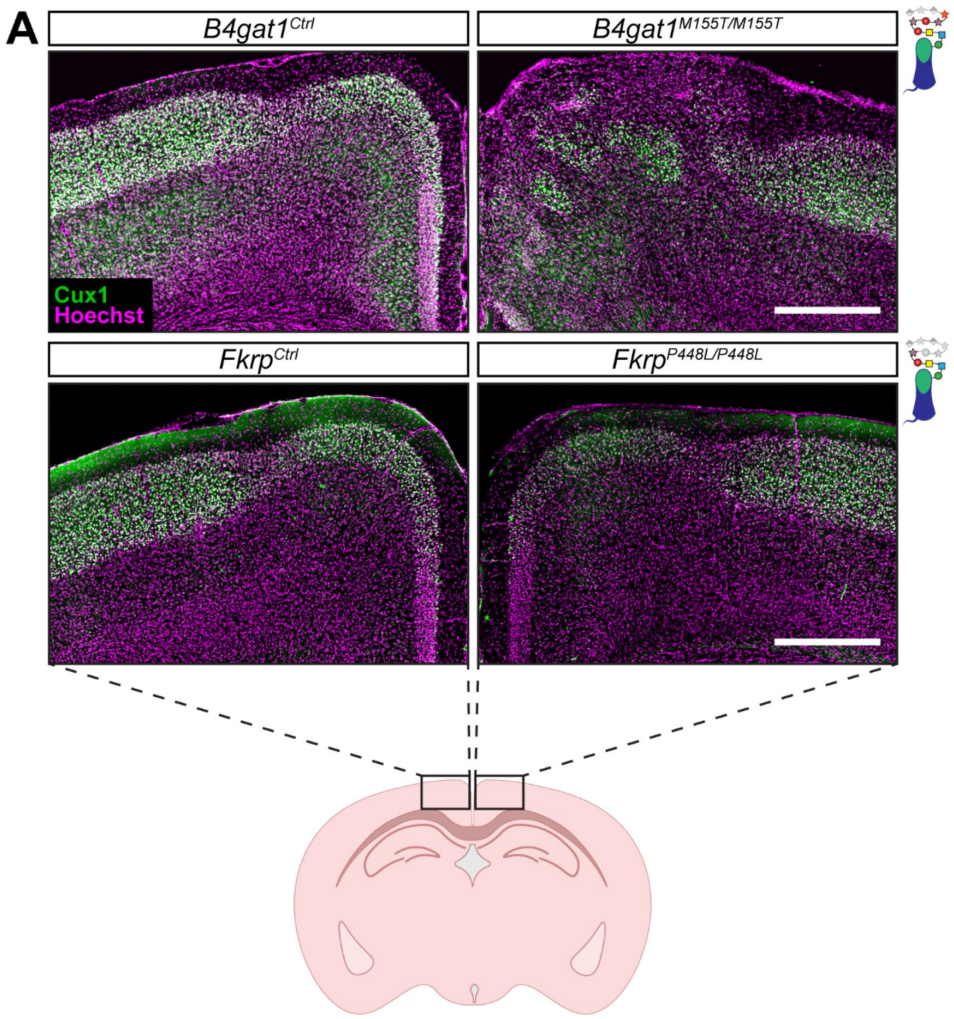

Figure 2 Supplement 1.

Cortical migration is disrupted at midline of *B4gat1*$^{M155T/M155T}$ but not *Fkrp*$^{P448L/P448L}$ mutants.

(A) Immunostaining for cortical layer marker Cux1 (layers 2-4) in P30 somatosensory cortex (scale bar = 500μm). Cux1 is shown in green. Nuclear marker Hoechst is shown in magenta. Cortical migration is normal in both *B4gat1* and *Fkrp* point mutants except at midline, where the *B4gat1* mutants show a migration phenotype not seen in the *Fkrp* point mutants. This phenotype was observed with 100% penetrance in the *B4gat1* mutants and 0% in the *Fkrp* mutants.

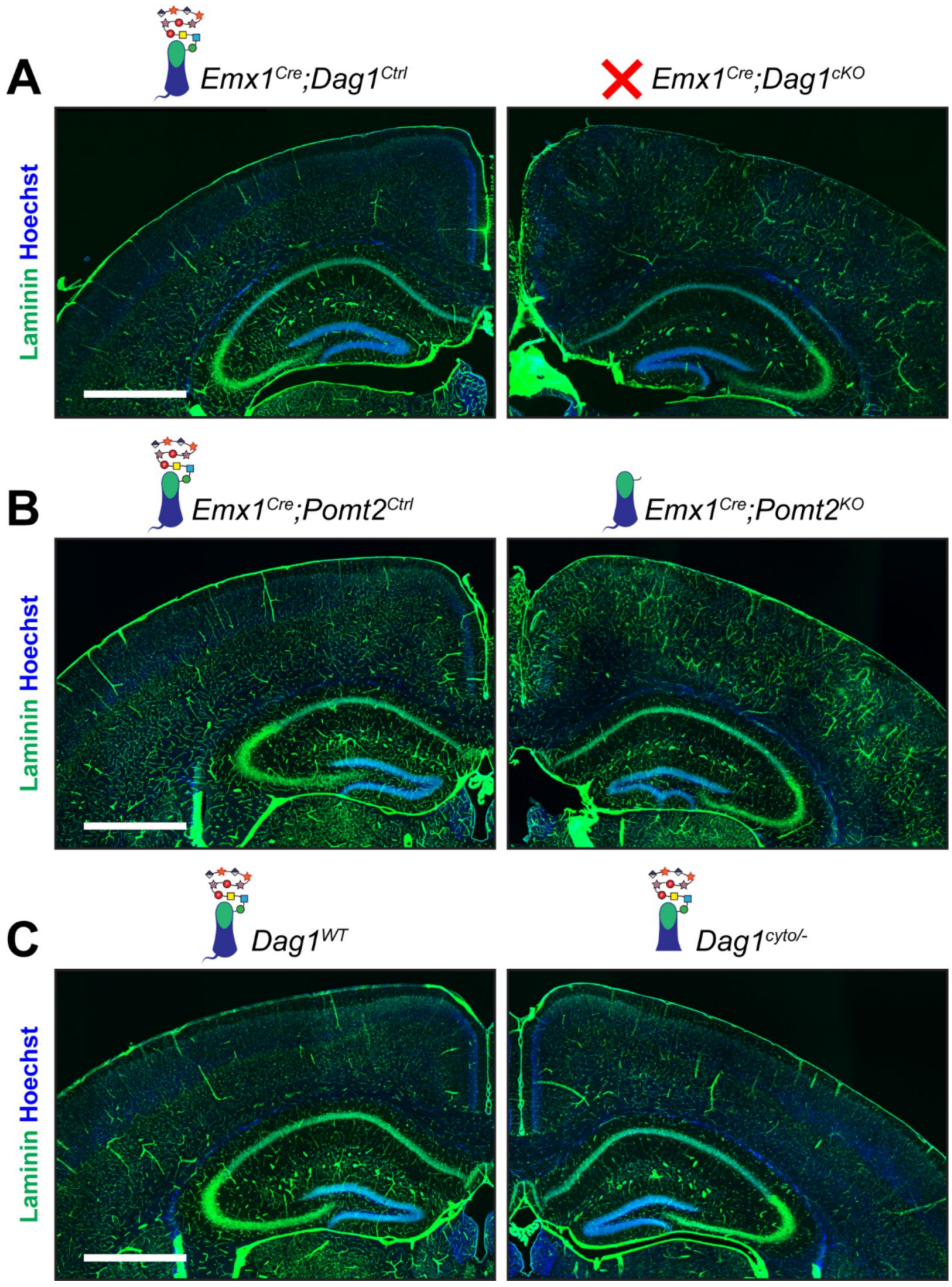

Figure 2 Supplement 2.

Laminin immunoreactivity in adult neocortex appears discontinuous in *Dag1* mutants. (A-C)

Immunostaining for ECM protein Laminin (green). Nuclear marker Hoechst is shown in blue. Scale bar = 1000μm.

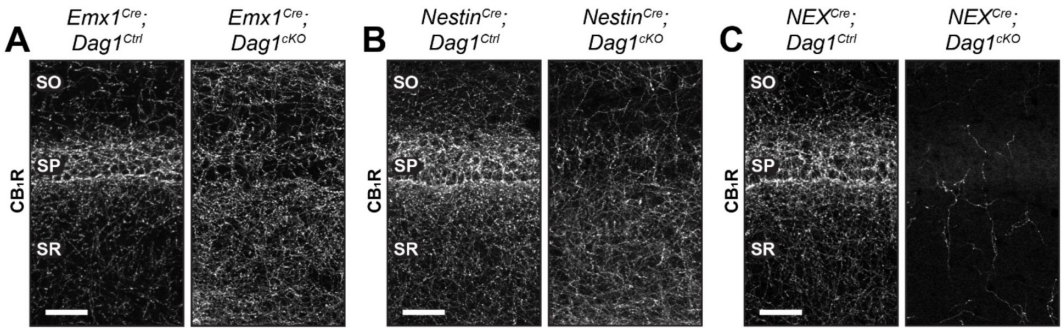

Figure 3 Supplement 1.

CCK^{+}/CB1R^{+} IN axon targeting phenotypes in hippocampal CA1 of various *Dag1^{cKOs}*.

CB1R immunostaining in hippocampal CA1 of control mice (left panels) and *Dag1^{cKOs}*(right panels) generated using *Emx1^{Cre}* (forebrain progenitors, E10.5) **(A)**, *Nestin^{Cre}*(neural stem cells in the central and peripheral nervous systems, E11.5) **(B)**, and *NEX^{Cre}* (forebrain postmitotic excitatory neurons, E12.5) **(C)**. Scale bar = 50μm. *Abbreviations: SO, stratum oriens; SP, stratum pyramidale; SR, stratum radiatum*.

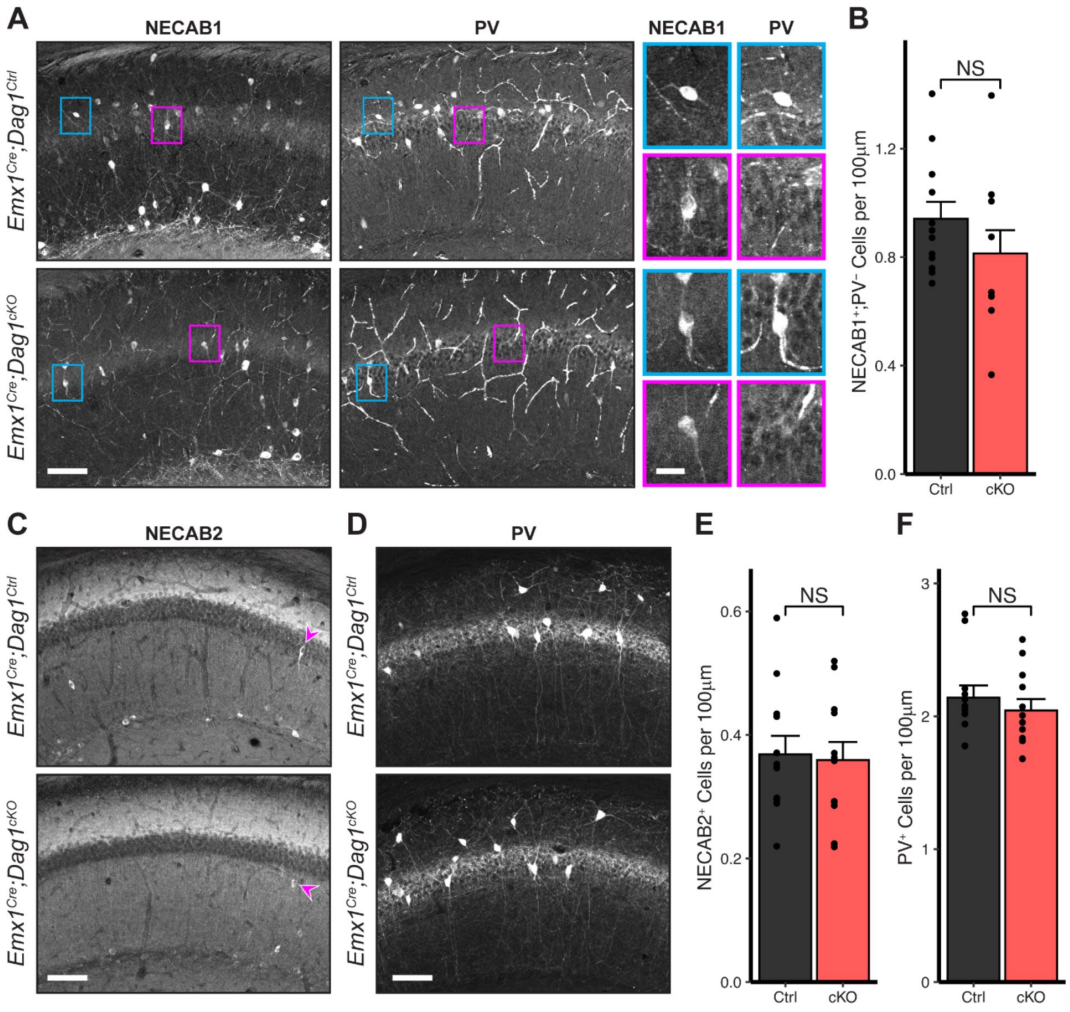

Figure 3 Supplement 2.

CCK$^+$/CB1R$^+$ IN cell numbers are unchanged in *Emx1^{Cre};Dag1^{cKOs}*.

(A) Immunostaining in hippocampal CA1 for NECAB1 (left) and PV (right) in *Emx1^{Cre};Dag1^{Ctrl}* and *Emx1^{Cre};Dag1^{cKO}* mice. NECAB1 labeling is evident in PV$^+$ cells (example shown in blue inset) and in an additional PV$^-$ population that contains the CCK$^+$/CB1R$^+$ population (example shown in magenta inset). The average number of NECAB1$^+$;PV$^-$ cells per 100µm of SP is quantified in **(B)**. Immunostaining for NECAB2 **(C)** and PV **(D)** with cell number quantification in **(E)** and **(F)**. Scale bar = 100µm. Error bars show mean + SEM. See **Supplementary Table 1** for Ns. *Significance: * = $p < 0.05$, ** = $p < 0.01$, *** = $p < 0.001$, NS = $p \geq 0.05$. Abbreviations: SP, stratum pyramidale; PV, parvalbumin*.

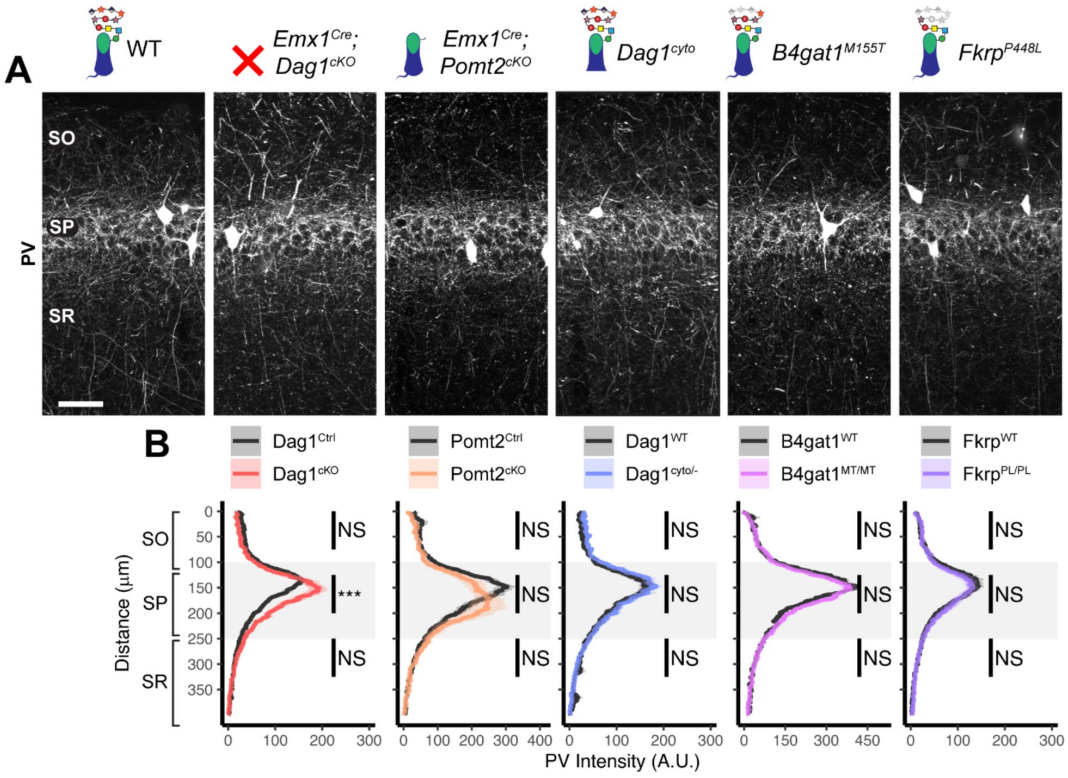

Figure 3 Supplement 3.

Parvalbumin^{+} basket INs do not require *Dag1* for proper axon targeting in hippocampal CA1.

(A) Parvalbumin (PV) immunostaining in P30 hippocampal CA1 shows that PV^{+} basket interneurons exhibit normal distribution in CA1 for all genetic models except for an increase in PV intensity within *stratum pyramidale* of *Emx1^{Cre};Dag1^{cKOs}* (scale bar = 50µm). **(B)** Quantification of CA1 PV fluorescence intensity profile. Shaded regions of intensity profile illustrate ± SEM. Gray region highlights SP. See **Supplementary Table 1** for Ns. *Significance: * = p < 0.05, ** = p < 0.01, *** = p < 0.001, NS = p ≥ 0.05. Abbreviations: A.U., arbitrary units; SO, stratum oriens; SP, stratum pyramidale; SR, stratum radiatum*.

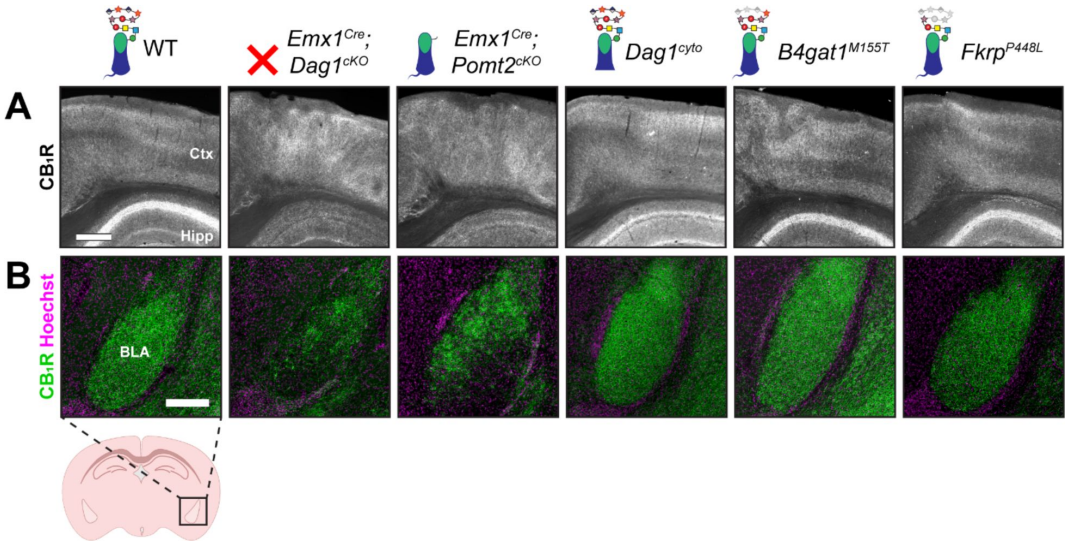

Figure 3 Supplement 4.

Altered CB1R expression in cortex and basolateral amygdala of *Dag1* and *POMT2* mutants.

(A) CB1R immunostaining in P30 coronal sections showing somatosensory cortex (Ctx) and CA1 of hippocampus (Hipp) (scale bar = 400μm). **(B)** CB1R immunostaining (green) shown with nuclear marker Hoechst (magenta) in basolateral amygdala (BLA) (scale bar = 250μm).

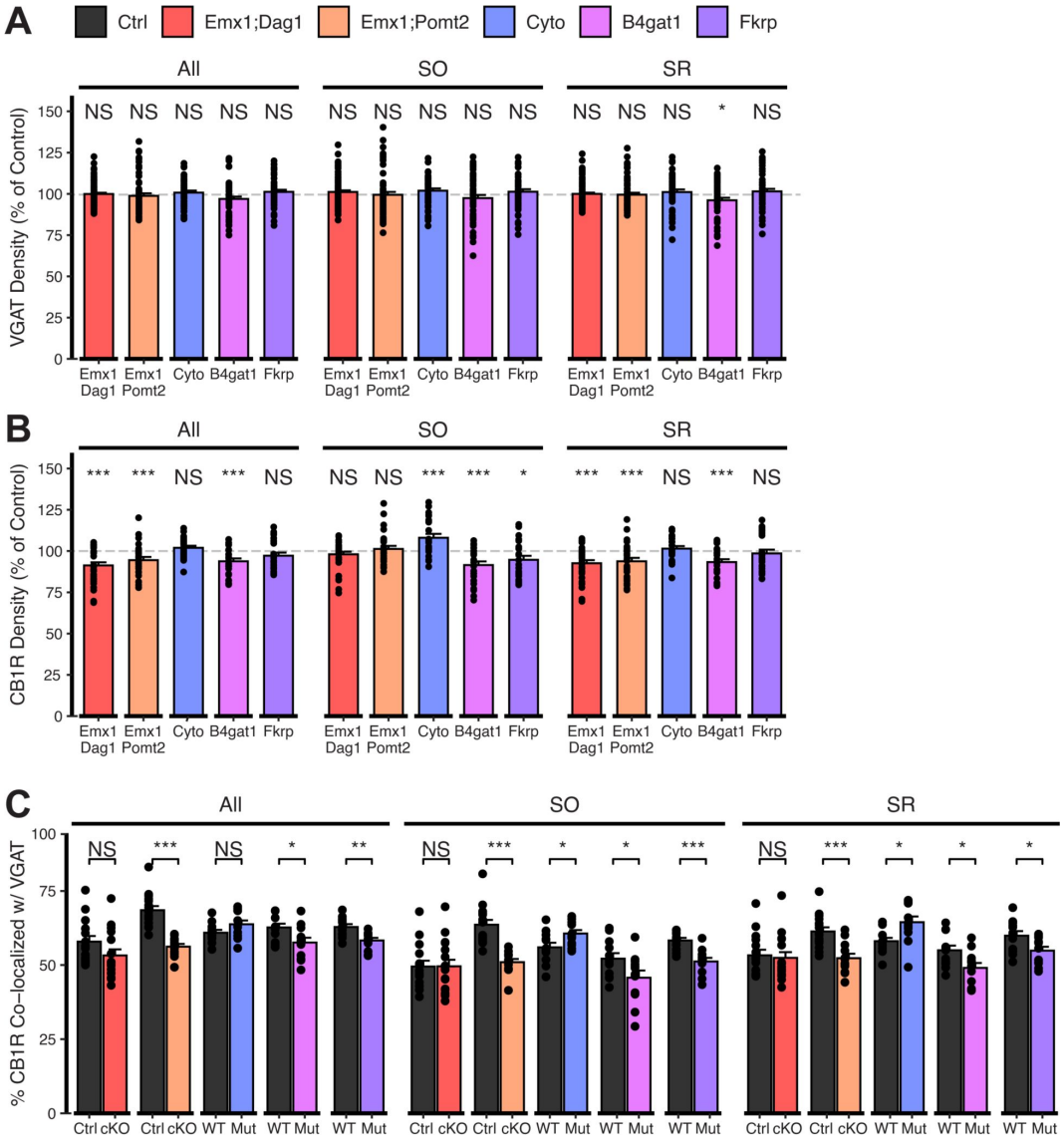

Figure 5 Supplement 1.

Extended quantification of images in Figure 5A-C.

Quantification within hippocampal CA1 SO and SR regions and all regions pooled together. **(A)** Quantification of VGAT puncta density expressed as a percent of control. **(B)** Quantification of CB1R puncta density expressed as a percent of control. **(C)** Quantification of co-localization between VGAT and CB1R to estimate putative CB1R^{+} basket cell synapse formation. Error bars show mean + SEM. (To see quantification of puncta densities and co-localization in SP see **Fig. 5D-F**.) See **Supplementary Table 1** for Ns. *Significance: * = p < 0.05, ** = p < 0.01, *** = p < 0.001, NS = p ≥ 0.05. Abbreviations: SO, stratum oriens; SP, stratum pyramidale; SR, stratum radiatum*.

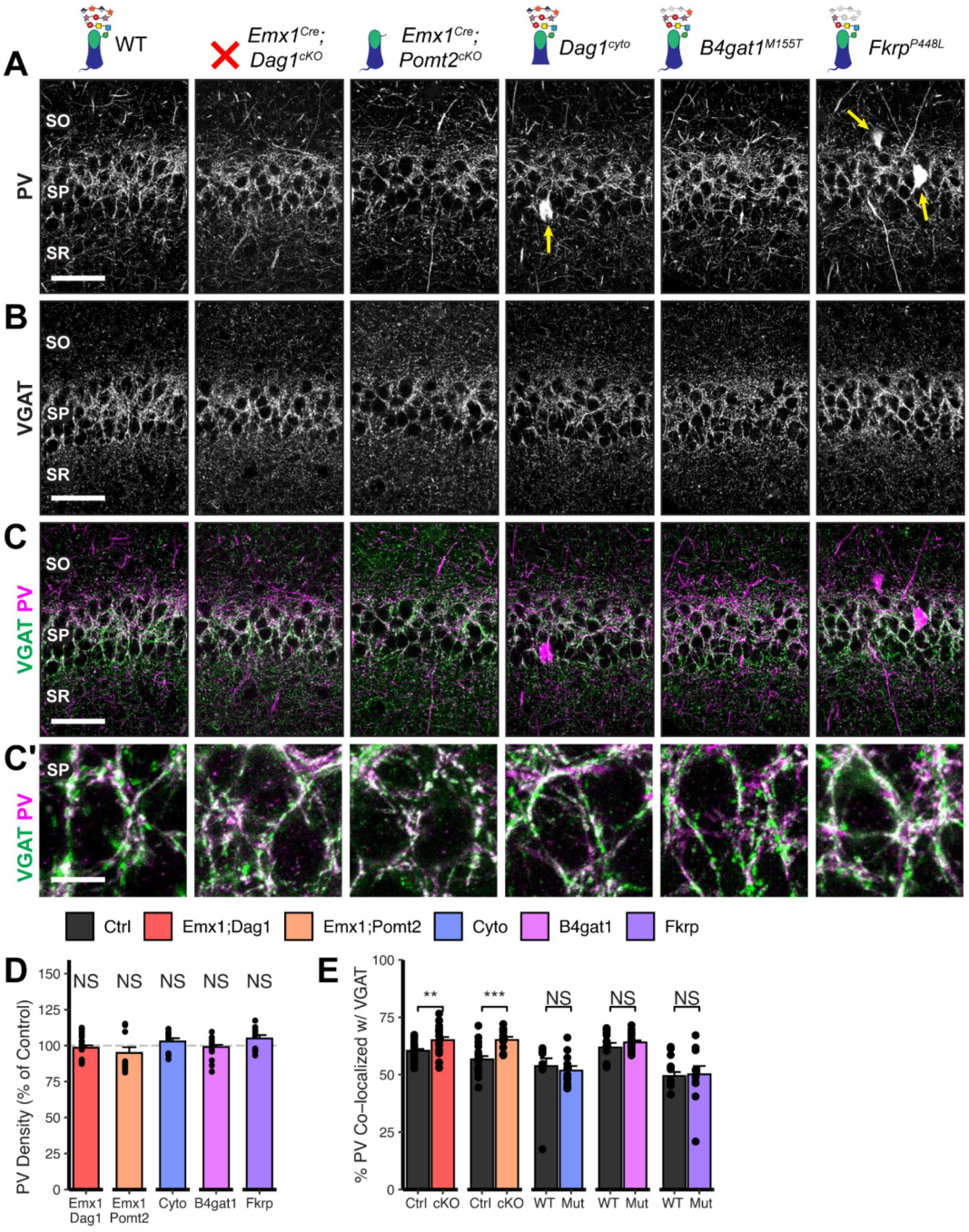

Figure 5 Supplement 2.

Dag1 and *Pomt2* cKOs exhibit increased PV$^+$ basket synapse formation in *stratum pyramidale* of hippocampal CA1.

P30 coronal sections immunostained for **(A)** PV and **(B)** VGAT in hippocampal CA1; merged image in **(C)** shows PV in magenta and VGAT in green. Yellow arrows indicate PV$^+$ interneuron cell bodies. (A-C) Scale bar = 50μm. (Higher magnification view of SP in **(C')**; scale bar = 10μm.) **(D)** Quantification of PV puncta density in SP expressed as a percent of control. **(E)** Quantification of co-localization between VGAT and PV in SP to estimate putative PV$^+$ basket synapse formation. Error bars show mean + SEM. (To see quantification of puncta densities and co-localization in SO and SR see **Fig. 5 Supp. 2**.) See **Supplementary Table 1** for Ns. *Significance: * = p < 0.05, ** = p < 0.01, *** = p < 0.001, NS = p ≥ 0.05. Abbreviations: PV, parvalbumin; SO, stratum oriens; SP, stratum pyramidale; SR, stratum radiatum*.

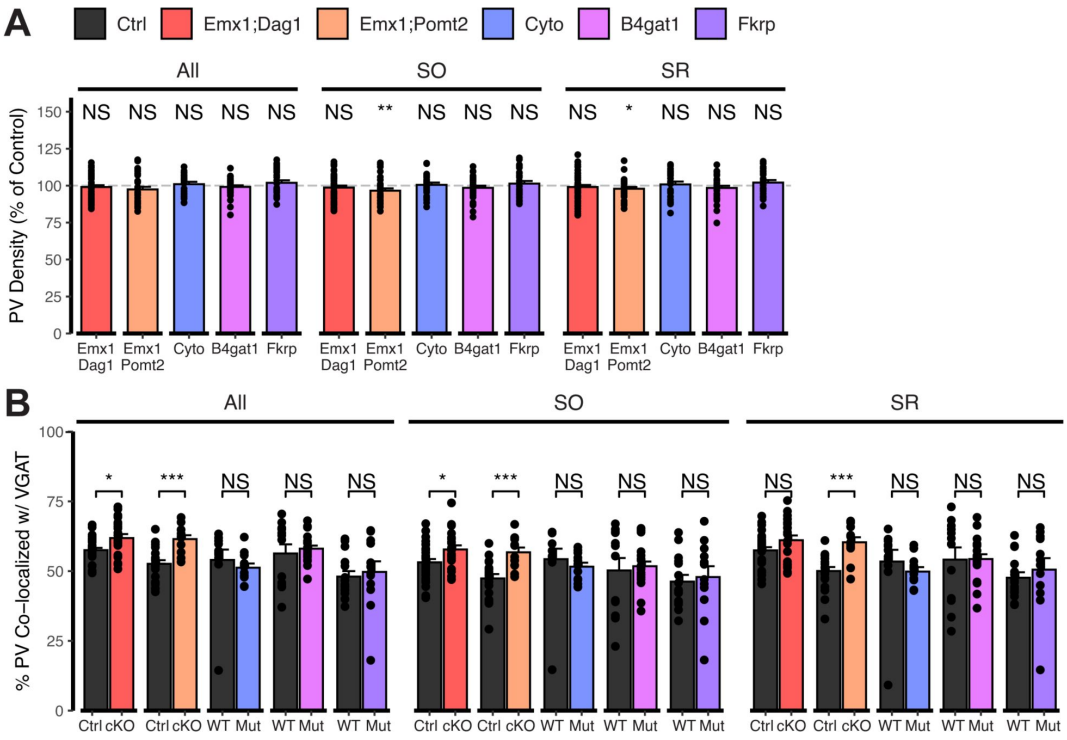

Figure 5 Supplement 3.

Extended quantification of images in Fig. 5 Supp. 2A-C.

Quantification within hippocampal CA1 SO and SR regions and all regions pooled together. **(A)** Quantification of PV puncta density expressed as a percent of control. **(B)** Quantification of co-localization between VGAT and PV to estimate putative PV^{+} basket cell synapse formation. Error bars show mean + SEM. (To see quantification of puncta densities and co-localization in SP see **Fig. 5 Supp. 2D-E**.) See **Supplementary Table 1** for Ns. *Significance: * = $p < 0.05$, ** = $p < 0.01$, *** = $p < 0.001$, NS = $p \geq 0.05$. Abbreviations: PV, parvalbumin; SO, stratum oriens; SP, stratum pyramidale; SR, stratum radiatum*.

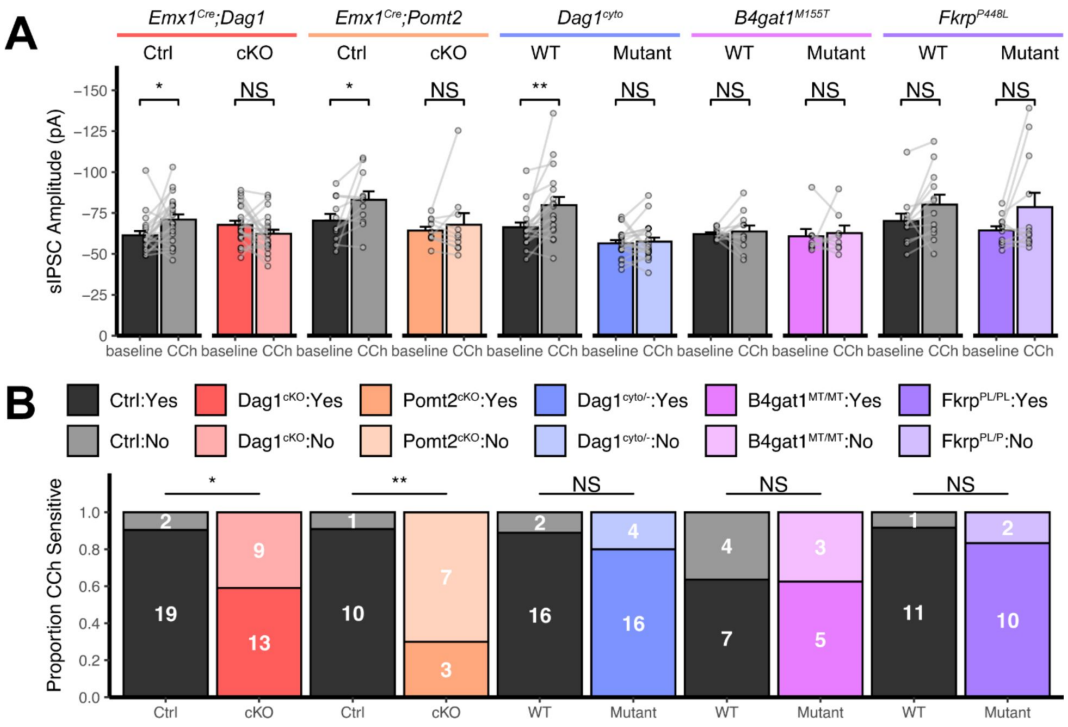

Figure 6 Supplement 1.

Additional quantification of sIPSC recordings.

(A) Quantification of average sIPSC amplitude at baseline and after the addition of carbachol. Error bars show mean + SEM. **(B)** Quantification of the proportion of carbachol-sensitive cells within each genotype. Non-responsive cells are shown in lighter color, responsive cells are shown in darker color. See **Supplementary Table 1** for Ns. *Significance: * = p < 0.05, ** = p < 0.01, *** = p < 0.001, NS = p ≥ 0.05. Abbreviations: sIPSC, spontaneous inhibitory postsynaptic current; CCh, carbachol*.

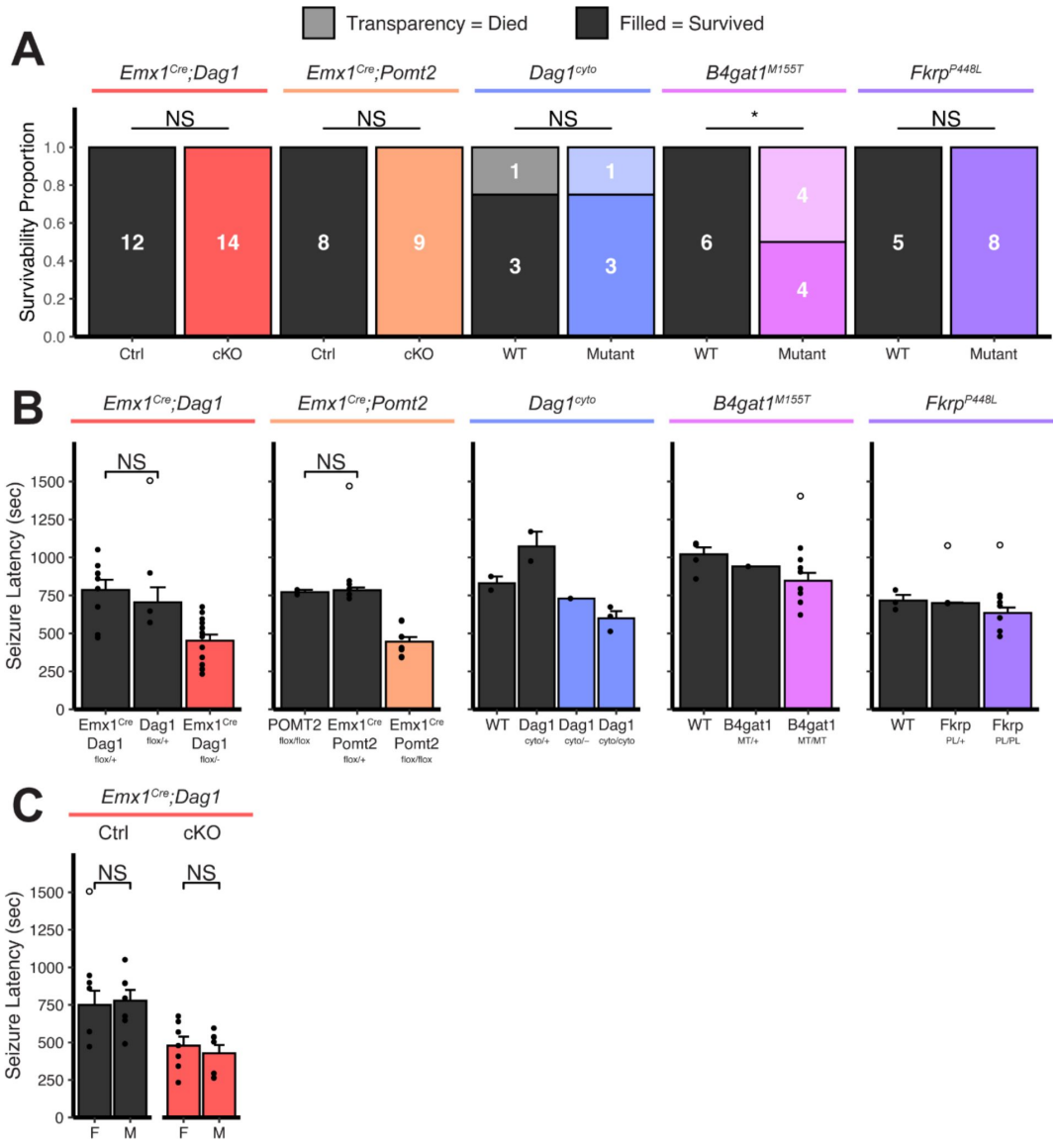

Figure 7 Supplement 1.

Extended seizure induction threshold data.

(A) Proportion of mice that died as a direct result of a flurothyl-induced seizure. Survivors are depicted in darker colors, fatalities in lighter colors. **(B)** To minimize the number of animals needed for this experiment, certain genotypes were pooled together. Here we show that pooled genotypes are not different. Statistical tests were run where Ns were sufficient to provide meaningful comparison. **(C)** Seizure latencies split by sex. Note: only the *Emx1^{Cre};Dag1* group is powered sufficiently to statistically compare sexes. Open points denote statistical outliers. Error bars show mean + SEM.

References

Barresi R., Campbell K. P (2006) **Dystroglycan: From biosynthesis to pathogenesis of human disease** *Journal of Cell Science* **119**:199–207 https://doi.org/10.1242/jcs.02814

Beedle A. M., Turner A. J., Saito Y., Lueck J. D., Foltz S. J., Fortunato M. J., Nienaber P. M., Campbell K. P (2012) **Mouse fukutin deletion impairs dystroglycan processing and recapitulates muscular dystrophy** *The Journal of Clinical Investigation* **122**:3330–3342 https://doi.org/10.1172/JCI63004

Berghuis P. *et al.* (2007) **Hardwiring the brain: Endocannabinoids shape neuronal connectivity. Science (New York** *N.Y* **316**:1212–1216 https://doi.org/10.1126/science.1137406

Blaeser A., Keramaris E., Chan Y. M., Sparks S., Cowley D., Xiao X., Lu Q. L (2013) **Mouse models of fukutin-related protein mutations show a wide range of disease phenotypes** *Human Genetics* **132**:923–934 https://doi.org/10.1007/s00439-013-1302-7

Boucard A. A., Chubykin A. A., Comoletti D., Taylor P., Südhof T. C (2005) **A Splice Code for trans-Synaptic Cell Adhesion Mediated by Binding of Neuroligin 1 to α- and β-Neurexins** *Neuron* **48**:229–236 https://doi.org/10.1016/j.neuron.2005.08.026

Briatore F., Patrizi A., Viltono L., Sassoe-Pognetto M., Wulff P (2010) **Quantitative organization of GABAergic synapses in the molecular layer of the mouse cerebellar cortex** *PLoS ONE* **5** https://doi.org/10.1371/journal.pone.0012119

Briatore F., Pregno G., Di Angelantonio S., Frola E., De Stefano M. E., Vaillend C., Sassoè-Pognetto M., Patrizi A. (2020) **Dystroglycan Mediates Clustering of Essential GABAergic Components in Cerebellar Purkinje Cells** *Frontiers in Molecular Neuroscience* **13** https://doi.org/10.3389/fnmol.2020.00164

Brockington M. *et al.* (2001) **Mutations in the Fukutin-Related Protein Gene (FKRP) Cause a Form of Congenital Muscular Dystrophy with Secondary Laminin α2 Deficiency and Abnormal Glycosylation of α-Dystroglycan** *The American Journal of Human Genetics* **69**:1198–1209 https://doi.org/10.1086/324412

Brünig I., Suter A., Knuesel I., Lüscher B., Fritschy J. M (2002) **GABAergic Terminals Are Required for Postsynaptic Clustering of Dystrophin but Not of GABAA Receptors and Gephyrin** *Journal of Neuroscience* **22**:4805–4813 https://doi.org/10.1523/jneurosci.22-12-04805.2002

Cataldi M. P., Blaeser A., Lu P., Leroy V., Lu Q. L (2020) **ISPD Overexpression Enhances Ribitol-Induced Glycosylation of α-Dystroglycan in Dystrophic FKRP Mutant Mice** *Molecular Therapy - Methods & Clinical Development* **17**:271–280 https://doi.org/10.1016/j.omtm.2019.12.005

Cataldi M. P., Lu P., Blaeser A., Lu Q. L (2018) **Ribitol restores functionally glycosylated α-dystroglycan and improves muscle function in dystrophic FKRP-mutant mice** *Nature Communications* **9** https://doi.org/10.1038/s41467-018-05990-z

Chan Y. M. *et al.* (2010) **Fukutin-related protein is essential for mouse muscle, brain and eye development and mutation recapitulates the wide clinical spectrums of dystroglycanopathies** *Human Molecular Genetics* **19**:3995–4006 https://doi.org/10.1093/hmg/ddq314

Chen L. Y., Jiang M., Zhang B., Gokce O., Südhof T. C (2017) **Conditional Deletion of All Neurexins Defines Diversity of Essential Synaptic Organizer Functions for Neurexins** *Neuron* **94**:611–625 https://doi.org/10.1016/j.neuron.2017.04.011

Clement E. *et al.* (2008) **Brain involvement in muscular dystrophies with defective dystroglycan glycosylation** *Annals of Neurology* **64**:573–582 https://doi.org/10.1002/ana.21482

Cohn R. D. *et al.* (2002) **Disruption of Dag1 in differentiated skeletal muscle reveals a role for dystroglycan in muscle regeneration** *Cell* **110**:639–648 https://doi.org/10.1016/S0092-8674(02)00907-8

Colognato H., Galvin J., Wang Z., Relucio J., Nguyen T., Harrison D., Yurchenco P. D., Ffrench-Constant C (2007) **Identification of dystroglycan as a second laminin receptor in oligodendrocytes, with a role in myelination** *Development* **134**:1723–1736 https://doi.org/10.1242/dev.02819

Dhaibani M. A. A., El-Hattab A. W., Ismayl O., Suleiman J (2018) **B3GALNT2- Related Dystroglycanopathy: Expansion of the Phenotype with Novel Mutation Associated with Muscle-Eye-Brain Disease, Walker–Warburg Syndrome, Epileptic Encephalopathy-West Syndrome, and Sensorineural Hearing Loss** *Neuropediatrics* **49**:289–295 https://doi.org/10.1055/s-0038-1651519

Di Rosa G., Messina S., D'Amico A., Bertini E., Pustorino G., Spanò M., Tortorella G. (2011) **A new form of alpha-dystroglycanopathy associated with severe drug-resistant epilepsy and unusual EEG features** *Epileptic Disorders* **13**:259–262 https://doi.org/10.1684/epd.2011.0461

Dudanova I., Tabuchi K., Rohlmann A., Südhof T. C., Missler M (2007) **Deletion of α-neurexins does not cause a major impairment of axonal pathfinding or synapse formation** *Journal of Comparative Neurology* **502**:261–274 https://doi.org/10.1002/cne.21305

Durbeej M., Henry M. D., Ferletta M., Campbell K. P., Ekblom P (1998) **Distribution of dystroglycan in normal adult mouse tissues** *Journal of Histochemistry and Cytochemistry* **46**:449–457 https://doi.org/10.1177/002215549804600404

Egawa K., Nakakubo S., Kimura S., Goto T., Manabe A., Shiraishi H (2021) **Flurothyl-induced seizure paradigm revealed higher seizure susceptibility in middle-aged Angelman syndrome mouse model** *Brain and Development* **43**:515–520 https://doi.org/10.1016/j.braindev.2020.12.011

Eggan S. M., Mizoguchi Y., Stoyak S. R., Lewis D. A (2010) **Development of Cannabinoid 1 Receptor Protein and Messenger RNA in Monkey Dorsolateral Prefrontal Cortex** *Cerebral Cortex* **20**:1164–1174 https://doi.org/10.1093/cercor/bhp179

Ervasti J. M., Campbell K. P (1991) **Membrane organization of the dystrophin-glycoprotein complex** *Cell* **66**:1121–1131 https://doi.org/10.1016/0092-8674(91)90035-W

Favuzzi E. *et al.* (2019) **Distinct molecular programs regulate synapse specificity in cortical inhibitory circuits** *Science* **363**:413–417 https://doi.org/10.1126/science.aau8977

Földy C., Neu A., Jones M. V., Soltesz I (2006) **Presynaptic, activity-dependent modulation of cannabinoid type 1 receptor-mediated inhibition of GABA release** *The Journal of Neuroscience: The Official Journal of the Society for Neuroscience* **26**:1465–1469 https://doi.org/10.1523/JNEUROSCI.4587-05.2006

Freund T. F., Katona I (2007) **Perisomatic inhibition** *Neuron* **56**:33–42 https://doi.org/10.1016/j.neuron.2007.09.012

Früh S., Romanos J., Panzanelli P., Bürgisser D., Tyagarajan S. K., Campbell K. P., Santello M., Fritschy J. M (2016) **Neuronal dystroglycan is necessary for formation and maintenance of functional CCK-positive basket cell terminals on pyramidal cells** *Journal of Neuroscience* **36**:10296–10313 https://doi.org/10.1523/JNEUROSCI.1823-16.2016

Fuccillo M. V., Földy C., Gökce Ö., Rothwell P. E., Sun G. L., Malenka R. C., Südhof T. C (2015) **Single-Cell mRNA Profiling Reveals Cell-Type-Specific Expression of Neurexin Isoforms** *Neuron* **87**:326–340 https://doi.org/10.1016/j.neuron.2015.06.028

Gerin I. *et al.* (2016) **ISPD produces CDP-ribitol used by FKTN and FKRP to transfer ribitol phosphate onto α- dystroglycan** *Nature Communications* **7** https://doi.org/10.1038/ncomms11534

Godfrey C. *et al.* (2007) **Refining genotype–phenotype correlations in muscular dystrophies with defective glycosylation of dystroglycan** *Brain* **130**:2725–2735 https://doi.org/10.1093/brain/awm212

Goebbels S., Bormuth I., Bode U., Hermanson O., Schwab M. H., Nave K.-A (2006) **Genetic targeting of principal neurons in neocortex and hippocampus of NEX-Cre mice** *Genesis* **44**:611–621 https://doi.org/10.1002/dvg.20256

Gorski J. A., Talley T., Qiu M., Puelles L., Rubenstein J. L. R., Jones K. R (2002) **Cortical Excitatory Neurons and Glia, But Not GABAergic Neurons** *Are Produced in the Emx* https://doi.org/10.1523/JNEUROSCI.22-15-06309.2002

Gu B., Levine N. G., Xu W., Lynch R. M., Pardo-Manuel de Villena F., Philpot B. D (2022) **Ictal neural oscillatory alterations precede sudden unexpected death in epilepsy** *Brain Communications* **4** https://doi.org/10.1093/braincomms/fcac073

Holt K. H., Crosbie R. H., Venzke D. P., Campbell K. P (2000) **Biosynthesis of dystroglycan: Processing of a precursor propeptide** *FEBS Letters* **468**:79–83 https://doi.org/10.1016/S0014-5793(00)01195-9

Holzfeind P. J., Grewal P. K., Reitsamer H. A., Kechvar J., Lassmann H., Hoeger H., Hewitt J. E., Bittner R. E (2002) **Skeletal, cardiac and tongue muscle pathology, defective retinal transmission, and neuronal migration defects in the Largemyd mouse defines a natural model for glycosylation-deficient muscle – eye – brain disorders** *Human Molecular Genetics* **11**:2673–2687 https://doi.org/10.1093/hmg/11.21.2673

Hu H., Li J., Gagen C. S., Gray N. W., Zhang Z., Qi Y., Zhang P (2011) **Conditional knockout of protein O-mannosyltransferase 2 reveals tissue-specific roles of O-mannosyl glycosylation in brain development** *Journal of Comparative Neurology* **519**:1320–1337 https://doi.org/10.1002/cne.22572

Hu H., Liu Y., Bampoe K., He Y., Yu M (2016) **Postnatal Gene Therapy Improves Spatial Learning Despite the Presence of Neuronal Ectopia in a Model of Neuronal Migration Disorder** *Genes* **7** https://doi.org/10.3390/genes7120105

Ibraghimov-Beskrovnaya O., Ervasti J. M., Leveille C. J., Slaughter C. A., Sernett S. W., Campbell K. P (1992) **Primary structure of dystrophin-associated glycoproteins linking dystrophin to the extracellular matrix** *Nature* **355**:696–702 https://doi.org/10.1038/355696a0

Jagadha V., Becker L. E (1988) **Brain morphology in Duchenne muscular dystrophy: A Golgi study** *Pediatric Neurology* **4**:87–92 https://doi.org/10.1016/0887-8994(88)90047-1

Jahncke J. N., Wright K. M (2023) **The many roles of dystroglycan in nervous system development and function** *Developmental Dynamics* **252**:61–80 https://doi.org/10.1002/dvdy.516

Kadiyala S. B., Yannix J. Q., Nalwalk J. W., Papandrea D., Beyer B. S., Herron B. J., Ferland R. J (2016) **Eight Flurothyl-Induced Generalized Seizures Lead to the Rapid Evolution of Spontaneous Seizures in Mice: A Model of Epileptogenesis with Seizure Remission** *Journal of Neuroscience* **36**:7485–7496 https://doi.org/10.1523/JNEUROSCI.3232-14.2016

Kanagawa M (2021) **Dystroglycanopathy: From Elucidation of Molecular and Pathological Mechanisms to Development of Treatment Methods** *International Journal of Molecular Sciences* **22** https://doi.org/10.3390/ijms222313162

Katona I., Rancz E. A., Acsady L., Ledent C., Mackie K., Hajos N., Freund T. F (2001) **Distribution of CB1 cannabinoid receptors in the amygdala and their role in the control of GABAergic transmission** *The Journal of Neuroscience: The Official Journal of the Society for Neuroscience* **21**:9506–9518 https://doi.org/10.1523/JNEUROSCI.21-23-09506.2001

Knuesel I., Mastrocola M., Zuellig R. A., Bornhauser B., Schaub M. C., Fritschy J. M (1999) **Altered synaptic clustering of GABAA receptors in mice lacking dystrophin (mdx mice)** *European Journal of Neuroscience* **11**:4457–4462 https://doi.org/10.1046/j.1460-9568.1999.00887.x

Krasowska E., Zabłocki K., Górecki D. C., Swinny J. D (2014) **Aberrant location of inhibitory synaptic marker proteins in the hippocampus of dystrophin-deficient mice: Implications for cognitive impairment in Duchenne muscular dystrophy** *PLoS ONE* **9** https://doi.org/10.1371/journal.pone.0108364

Larsen I. S. B. *et al.* (2017) **Mammalian O-mannosylation of cadherins and plexins is independent of protein O-mannosyltransferases 1 and 2** *Journal of Biological Chemistry* **292**:11586–11598 https://doi.org/10.1074/jbc.M117.794487

Lévi S., Grady R. M., Henry M. D., Campbell K. P., Sanes J. R., Craig A. M (2002) **Dystroglycan Is Selectively Associated with Inhibitory GABAergic Synapses but Is Dispensable for Their Differentiation** *Journal of Neuroscience* **22**:4274–4285 https://doi.org/10.1523/jneurosci.22-11-04274.2002

Liang H., Hippenmeyer S., Ghashghaei H. T (2012) **A Nestin-cre transgenic mouse is insufficient for recombination in early embryonic neural progenitors** *Biology Open* **1**:1200–1203 https://doi.org/10.1242/bio.20122287

Lin P.-Y., Chen L. Y., Jiang M., Trotter J. H., Seigneur E., Südhof T. C (2023) **Neurexin-2: An inhibitory neurexin that restricts excitatory synapse formation in the hippocampus** *Science Advances* **9** https://doi.org/10.1126/sciadv.add8856

Lindenmaier L. B., Parmentier N., Guo C., Tissir F., Wright K. M (2019) **Dystroglycan is a scaffold for extracellular axon guidance decisions** *eLife* **8** https://doi.org/10.7554/eLife.42143

Manya H., Chiba A., Yoshida A., Wang X., Chiba Y., Jigami Y., Margolis R. U., Endo T (2004) **Demonstration of mammalian protein O-mannosyltransferase activity: Coexpression of POMT1 and POMT2 required for enzymatic activity** *Proceedings of the National Academy of Sciences* **101**:500–505 https://doi.org/10.1073/pnas.0307228101

Meilleur K. G. *et al.* (2014) **Clinical, pathologic, and mutational spectrum of dystroglycanopathy caused by LARGE mutations** *Journal of Neuropathology and Experimental Neurology* **73**:425–441 https://doi.org/10.1097/NEN.0000000000000065

Menezes M. J., McClenahan F. K., Leiton C. V., Aranmolate A., Shan X., Colognato H (2014) **The extracellular matrix protein laminin α2 regulates the maturation and function of the blood–brain barrier** *Journal of Neuroscience* **34**:15260–15280 https://doi.org/10.1523/JNEUROSCI.3678-13.2014

Mercuri E. *et al.* (2009) **Congenital muscular dystrophies with defective glycosylation of dystroglycan: A population study** *Neurology* **72**:1802–1809 https://doi.org/10.1212/01.wnl.0000346518.68110.60

Miczán V., Kelemen K., Glavinics J. R., László Z. I., Barti B., Kenesei K., Kisfali M., Katona I (2021) **NECAB1 and NECAB2 are Prevalent Calcium-Binding Proteins of CB1/CCK-Positive GABAergic Interneurons** *Cerebral Cortex* **31**:1786–1806 https://doi.org/10.1093/cercor/bhaa326

Miller D. S., Wright K. M (2021) **Neuronal Dystroglycan regulates postnatal development of CCK/cannabinoid receptor-1 interneurons** *Neural Development* **16** https://doi.org/10.1186/s13064-021-00153-1

Missler M., Zhang W., Rohlmann A., Kattenstroth G., Hammer R. E., Gottmann K., Südhof T. C (2003) **α-Neurexins couple Ca2+ channels to synaptic vesicle exocytosis** *Nature* **423** https://doi.org/10.1038/nature01755

Moizard M.-P., Toutain A., Fournier D., Berret F., Raynaud M., Billard C., Andres C., Moraine C (2000) **Severe cognitive impairment in DMD: Obvious clinical evidence for Dp71 isoform point mutations screening** *European Journal of Human Genetics* **8** https://doi.org/10.1038/sj.ejhg.5200488

Monory K., Polack M., Remus A., Lutz B., Korte M (2015) **Cannabinoid CB1 Receptor Calibrates Excitatory Synaptic Balance in the Mouse Hippocampus** *Journal of Neuroscience* **35**:3842–3850 https://doi.org/10.1523/JNEUROSCI.3167-14.2015

Moore C. J., Winder S. J (2010) **Dystroglycan versatility in cell adhesion: A tale of multiple motifs** *Cell Communication and Signaling* **8** https://doi.org/10.1186/1478-811X-8-3

Moore S. A. *et al.* (2002) **Deletion of brain dystroglycan recapitulates aspects of congenital muscular dystrophy** *Nature* **418**:422–425 https://doi.org/10.1038/nature00838

Morozov Y. M., Freund T. F (2003) **Postnatal development and migration of cholecystokinin-immunoreactive interneurons in rat hippocampus** *Neuroscience* **120**:923–939 https://doi.org/10.1016/S0306-4522(03)00409-3

Morozov Y. M., Freund T. F (2003) **Post-natal development of type 1 cannabinoid receptor immunoreactivity in the rat hippocampus** *The European Journal of Neuroscience* **18**:1213–1222 https://doi.org/10.1046/j.1460-9568.2003.02852.x

Morozov Y. M., Torii M., Rakic P (2009) **Origin, Early Commitment** *Migratory Routes, and Destination of Cannabinoid Type* **1** https://doi.org/10.1093/cercor/bhp028

Mulder J. *et al.* (2008) **Endocannabinoid signaling controls pyramidal cell specification and long-range axon patterning** *Proceedings of the National Academy of Sciences* **105**:8760–8765 https://doi.org/10.1073/pnas.0803545105

Muntoni F., Torelli S., Wells D. J., Brown S. C (2011) **Muscular dystrophies due to glycosylation defects: Diagnosis and therapeutic strategies** *Current Opinion in Neurology* **24**:437–442 https://doi.org/10.1097/WCO.0b013e32834a95e3

Myshrall T. D., Moore S. A., Ostendorf A. P., Satz J. S., Kowalczyk T., Nguyen H., Daza R. A. M., Lau C., Campbell K. P., Hevner R. F (2012) **Dystroglycan on radial glia end feet is required for pial basement membrane integrity and columnar organization of the developing cerebral cortex** *Journal of Neuropathology and Experimental Neurology* **71**:1047–1063 https://doi.org/10.1097/NEN.0b013e318274a128

Nagode D. A., Tang A.-H., Yang K., Alger B. E (2014) **Optogenetic identification of an intrinsic cholinergically driven inhibitory oscillator sensitive to cannabinoids and opioids in hippocampal CA1** *The Journal of Physiology* **592**:103–123 https://doi.org/10.1113/jphysiol.2013.257428

Naidoo M., Anthony K (2020) **Dystrophin Dp71 and the Neuropathophysiology of Duchenne Muscular Dystrophy** *Molecular Neurobiology* **57**:1748–1767 https://doi.org/10.1007/s12035-019-01845-w

Nguyen H., Ostendorf A. P., Satz J. S., Westra S., Ross-Barta S. E., Campbell K. P., Moore S. A (2014) **Glial scaffold required for cerebellar granule cell migration is dependent on dystroglycan function as a receptor for basement membrane proteins** *Acta Neuropathologica Communications* **2** https://doi.org/10.1186/2051-5960-1-58

Nickolls A. R., Bönnemann C. G (2018) **The roles of dystroglycan in the nervous system: Insights from animal models of muscular dystrophy** *DMM Disease Models and Mechanisms* **11** https://doi.org/10.1242/dmm.035931

Omori Y. *et al.* (2012) **Presynaptic dystroglycan-pikachurin complex regulates the proper synaptic connection between retinal photoreceptor and bipolar cells** *Journal of Neuroscience* **32**:6126–6137 https://doi.org/10.1523/JNEUROSCI.0322-12.2012

Orlandi C. *et al.* (2018) **Transsynaptic Binding of Orphan Receptor GPR179 to Dystroglycan-Pikachurin Complex Is Essential for the Synaptic Organization of Photoreceptors** *Cell Reports* **25**:130–145 https://doi.org/10.1016/j.celrep.2018.08.068

Patrizi A. *et al.* (2008) **Synapse formation and clustering of neuroligin-2 in the absence of GABAA receptors** *Proceedings of the National Academy of Sciences* **105**:13151–13156 https://doi.org/10.1073/pnas.0802390105

Pawlisz A. S., Feng Y (2011) **Three-dimensional regulation of radial glial functions by lis1-nde1 and dystrophin glycoprotein complexes** *PLoS Biology* **9** https://doi.org/10.1371/journal.pbio.1001172

Peron S. P., Freeman J., Iyer V., Guo C., Svoboda K (2015) **A Cellular Resolution Map of Barrel Cortex Activity during Tactile Behavior** *Neuron* **86**:783–799 https://doi.org/10.1016/j.neuron.2015.03.027

Raphael A. R., Couthouis J., Sakamuri S., Siskind C., Vogel H., Day J. W., Gitler A. D (2014) **Congenital Muscular Dystrophy and Generalized Epilepsy Caused by GMPPB Mutations** *Brain Research* **0**:66–71 https://doi.org/10.1016/j.brainres.2014.04.028

Reeuwijk J. van *et al.* (2005) **POMT2 mutations cause α-dystroglycan hypoglycosylation and Walker-Warburg syndrome** *Journal of Medical Genetics* **42**:907–912 https://doi.org/10.1136/jmg.2005.031963

Reissner C., Stahn J., Breuer D., Klose M., Pohlentz G., Mormann M., Missler M (2014) **Dystroglycan binding to α-Neurexin competes with neurexophilin-1 and neuroligin in the brain** *Journal of Biological Chemistry* **289**:27585–27603 https://doi.org/10.1074/jbc.M114.595413

Rubio-Fernández M., Uribe M. L., Vicente-Tejedor J., Germain F., Susín-Lara C., Quereda C., Montoliu L., de la Villa P., Martín-Nieto J., Cruces J. (2018) **Impairment of photoreceptor ribbon synapses in a novel Pomt1 conditional knockout mouse model of dystroglycanopathy** *Scientific Reports* **8** https://doi.org/10.1038/s41598-018-26855-x

Satz J. S., Barresi R., Durbeej M., Willer T., Turner A., Moore S. A., Campbell K. P (2008) **Brain and eye malformations resembling Walker-Warburg syndrome are recapitulated in mice by dystroglycan deletion in the epiblast** *Journal of Neuroscience* **28**:10567–10575 https://doi.org/10.1523/JNEUROSCI.2457-08.2008

Satz J. S. *et al.* (2010) **Distinct functions of glial and neuronal dystroglycan in the developing and adult mouse brain** *Journal of Neuroscience* **30**:14560–14572 https://doi.org/10.1523/JNEUROSCI.3247-10.2010

Satz J. S. *et al.* (2009) **Visual impairment in the absence of dystroglycan** *Journal of Neuroscience* **29**:13136–13146 https://doi.org/10.1523/JNEUROSCI.0474-09.2009

Schindelin J. *et al.* (2012) **Nature Methods** https://doi.org/10.1038/nmeth.2019

Sheikh M. O. *et al.* (2022) **Cell surface glycan engineering reveals that matriglycan alone can recapitulate dystroglycan binding and function** *Nature Communications* **13** https://doi.org/10.1038/s41467-022-31205-7

Südhof T. C (2018) **Towards an Understanding of Synapse Formation** *Neuron* **100**:276–293 https://doi.org/10.1016/j.neuron.2018.09.040

Sugita S., Saito F., Tang J., Satz J., Campbell K., Südhof T. C (2001) **A stoichiometric complex of neurexins and dystroglycan in brain** *Journal of Cell Biology* **154**:435–445 https://doi.org/10.1083/jcb.200105003

Taniguchi-Ikeda M., Morioka I., Iijima K., Toda T (2016) **Mechanistic aspects of the formation of α-dystroglycan and therapeutic research for the treatment of α- dystroglycanopathy: A review** *Molecular Aspects of Medicine* **51**:115–124 https://doi.org/10.1016/j.mam.2016.07.003

Tian M., Jacobson C., Gee S. H., Campbell K. P., Carbonetto S., Jucker M (1996) **Dystroglycan in the cerebellum is a laminin α2-chain binding protein at the glial-vascular interface and is expressed in Purkinje cells** *European Journal of Neuroscience* **8**:2739–2747 https://doi.org/10.1111/j.1460-9568.1996.tb01568.x

Tronche F., Kellendonk C., Kretz O., Gass P., Anlag K., Orban P. C., Bock R., Klein R., Schütz G (1999) **Disruption of the glucocorticoid receptor gene in the nervous system results in reduced anxiety** *Nature Genetics* **23** https://doi.org/10.1038/12703

Trotter J. H., Wang C. Y., Zhou P., Nakahara G., Südhof T. C (2023) **A combinatorial code of neurexin-3 alternative splicing controls inhibitory synapses via a trans-synaptic dystroglycan signaling loop** *Nature Communications* **14** https://doi.org/10.1038/s41467-023-36872-8

Uezu A., Hisey E., Kobayashi Y., Gao Y., Bradshaw T. W. A., Devlin P., Rodriguiz R., Tata P. R., Soderling S. H (2019) **Essential role for insyn1 in dystroglycan complex integrity and cognitive behaviors in mice** *eLife* **8** https://doi.org/10.7554/eLife.50712

Ullrich B., Ushkaryov Y. A., Südhof T. C (1995) **Cartography of neurexins: More than 1000 isoforms generated by alternative splicing and expressed in distinct subsets of neurons** *Neuron* **14**:497–507 https://doi.org/10.1016/0896-6273(95)90306-2

Vitalis T., Lainé J., Simon A., Roland A., Leterrier C., Lenkei Z (2008) **The type 1 cannabinoid receptor is highly expressed in embryonic cortical projection neurons and negatively regulates neurite growth in vitro** *European Journal of Neuroscience* **28**:1705–1718 https://doi.org/10.1111/j.1460-9568.2008.06484.x

Wang J., Lin Z.-J., Liu L., Xu H.-Q., Shi Y.-W., Yi Y.-H., He N., Liao W.-P (2017) **Epilepsy-associated genes** *Seizure* **44**:11–20 https://doi.org/10.1016/j.seizure.2016.11.030

Willer T., Inamori K., Venzke D., Harvey C., Morgensen G., Hara Y., Beltrán Valero de Bernabé D., Yu L., Wright K. M., Campbell K. P. (2014) **The glucuronyltransferase B4GAT1 is required for initiation of LARGE-mediated α- dystroglycan functional glycosylation** *eLife* **3** https://doi.org/10.7554/eLife.03941

Wright K. M., Lyon K. A., Leung H., Leahy D. J., Ma L., Ginty D. D (2012) **Dystroglycan Organizes Axon Guidance Cue Localization and Axonal Pathfinding** *Neuron* **76**:931–944 https://doi.org/10.1016/j.neuron.2012.10.009

Yanagisawa A. *et al.* (2007) **New POMT2 mutations causing congenital muscular dystrophy: Identification of a founder mutation** *Neurology* **69**:1254–1260 https://doi.org/10.1212/01.wnl.0000268489.60809.c4

Yang H., Song D., Liu Y., Chen X., Zhu Y., Wei C., Fu X., Liu X., Yang Z., Xiong H (2022) **Seizures and EEG characteristics in a cohort of pediatric patients with dystroglycanopathies** *Seizure* **101**:39–47 https://doi.org/10.1016/j.seizure.2022.07.008

Yoshida-Moriguchi T., Campbell K. P (2015) **Matriglycan: A novel polysaccharide that links dystroglycan to the basement membrane** *Glycobiology* **25**:702–713 https://doi.org/10.1093/glycob/cwv021

Zaccaria M. L., Di Tommaso F., Brancaccio A., Paggi P., Petrucci T. C. (2001) **Dystroglycan distribution in adult mouse brain: A light and electron microscopy study** *Neuroscience* **104**:311–324 https://doi.org/10.1016/S0306-4522(01)00092-6

Article and author information

Jennifer N. Jahncke
Neuroscience Graduate Program, Oregon Health & Science University, Portland, OR 97239, USA
ORCID iD: 0000-0003-2319-6109

Daniel S. Miller
Neuroscience Graduate Program, Oregon Health & Science University, Portland, OR 97239, USA
ORCID iD: 0000-0001-5927-4397

Milana Krush
Neuroscience Graduate Program, Oregon Health & Science University, Portland, OR 97239, USA
ORCID iD: 0000-0003-4833-8564

Eric Schnell
Operative Care Division, Portland VA Health Care System, Anesthesiology and Perioperative Medicine, Oregon Health & Science University, Portland, OR 97239, USA
ORCID iD: 0000-0002-5623-5015

Kevin M. Wright
Vollum Institute, Oregon Health & Science University, Portland, OR 97239, USA
For correspondence: wrighke@ohsu.edu
ORCID iD: 0000-0001-5094-5270

Copyright

Editors

Reviewing Editor
Linda Overstreet-Wadiche
University of Alabama at Birmingham, United States of America

Senior Editor
Lu Chen
Stanford University, United States of America

Reviewer #1 (Public Review):

This important study from Jahncke et al. demonstrates inhibitory synaptic defects and elevated seizure susceptibility in multiple models of dystroglycanopathy. A strength of the paper is the use of a wide range of genetic models to disrupt different aspects of dystroglycan protein or glycosylation in forebrain neurons. The authors use a combination of immunohistochemistry and electrophysiology to identify cellular migration, lamination, axonal targeting, synapse formation/function, and seizure phenotypes in forebrain neurons.

This is an elegant study with extensive data supporting the conclusions. The role of dystroglycan and the dystrophin glycoprotein complex (DGC) in cellular migration and synapse formation are of broad interest.
A strength of this paper is the use of several transgenic mouse lines with mutations in genes involved in glycosylation of dystroglycan. Knockout of POMT2 abolishes the majority of dystroglycan glycosylation, while point mutations in B4GAT and FKRP presumably produce more minor changes in glycosylation. This is a powerful approach to investigate the role of glycosylation in dystroglycan function.

Reviewer #2 (Public Review):

The manuscript by Jahncke and colleagues is centered on the CCK+ synaptic defects that are a consequence of Dystroglycanopathy and/or impaired dystroglycan-related protein function. The authors use conditional mouse models for Dag1 and Pomt2 to ablate their function in mouse forebrain neurons and demonstrate significant impairment of CCK+/CB1R+ interneuron (IN) development in addition to being prone to seizures. Mice lacking the intracellular domain of Dystroglycan have milder defects, but impaired CCK+/CB1R+ IN axon targeting. The authors conclude that the milder dystroglycanopathy is due to the partially reduced glycosylation that occurs in the milder mouse models as opposed to the more severe Pomt2 models. Additionally, the authors postulate that inhibitory synaptic defects and elevated seizure susceptibility are hallmarks of severe dystroglycanopathy and are required for the organization of functional inhibitory synapse assembly.

The manuscript is overall, fairly well-written and the description of the phenotypic impact of disruption of Dystroglycan forebrain neurons (and similar glycosyltransferase pathway proteins) demonstrate impairment in axon targeting and organization. There are some questions with regards to interpretation of some of the results from these conditional mouse models. The study is mostly descriptive, and some validation of subunits of the dystroglycan-glycoprotein complex and laminin interactions would go towards defining the impact of disruption of dystroglycan's function in the brain. The statistics and basic analysis of the manuscript appear to be appropriate and within parameters for a study of this nature. Some clarification between the discrepancies between the Walker Warburg Syndrome (WWS) patient phenotypes and those observed in these conditional mouse models is warranted. This manuscript has the potential to be impactful in the Dystroglycanopathy and general neurobiology fields.

The authors have made significant improvements to address my concerns in this resubmission and the previous critiques of the other reviewers since the prior submission. The work is comprehensive in scope and the statistics are appropriate where required. I believe the conclusions to be valid for this study and I don't have any additional recommendations. I believe this work to be of importance to the Dystroglycanopathy and neurobiology fields.

Reviewer #3 (Public Review):

The study presents a systematic analysis of how a range of dystroglycan mutations alter CCK/CB1 axonal targeting and inhibition in hippocampal CA1 and impact seizure susceptibility. The study follows up on prior literature identifying a role for dystroglycan in CCK/CB1 synapse formation. The careful assay includes comparison of 5 distinct dystroglycan mutation types known to be associated with varying degrees of muscular dystrophy phenotypes: a forebrain specific Dag1 knockout in excitatory neurons at 10.5, a forebrain specific knockout of the glycosyltransferase enzyme in excitatory neurons, mice with deletion of the intracellular domain of beta-Dag1 and 2 lines with missense mutations with milder phenotypes. They show that forebrain glutamatergic deletion of Dag1 or glycosyltransferase alters cortical lamination while lamination is preserved in mice with deletion of the intracellular domain or missense mutation. The study extends prior works by identifying that

forebrain deletion of Dag1 or glycosyltransferase in excitatory neurons impairs CCK/CB1 and not PV axonal targeting and CB1 basket formation around CA1 pyramidal cells. Mice with deletion of the intracellular domain or missense mutation show
limited reductions in CCK/CB1 fibers in CA1. Carbachol enhancement of CA1 IPSCs was reduced both in forebrain knockouts. Interestingly, carbachol enhancement of CA1 IPSCs was reduced when the intracellular domain of beta-Dag1was deleted, but not I the missense mutations, suggesting a role of the intracellular domain in synapse maintenance. All lines except the missense mutations , showed increased susceptibility to chemically induced behavioral seizures. Together, the study, is carefully designed, well controlled and systematic. The results advance prior findings of the role for dystroglycans in CCK/CB1 innervations of PCs by demonstrating effects of more selective cellular deletions and site specific mutations in extracellular and intracellular domains.

Prior concerns regarding CCK/CB1 cell numbers and potential changes in basal synaptic inhibition are addressed in the revision.

Author Response

The following is the authors' response to the original reviews.

We thank the reviewers for their service and are pleased to see that they were positive about the overall study. The reviewers provided several very good suggestions that we feel have improved the revised manuscript. In response to their suggestions, we have added four new figures of additional data (Figure 1, Supplement 2; Figure 2, Supplement 2; Figure 3, Supplements 1 and 2) in this revision. We have addressed the specific review comments/suggestions point-by-point below. Text changes in the manuscript are indicated in red with line numbers indicated.

> ***Public Reviews:***
>
> ***Reviewer #1 (Public Review):***
>
> *This important study from Jahncke et al. demonstrates inhibitory synaptic defects and elevated seizure susceptibility in multiple models of dystroglycanopathy. A strength of the paper is the use of a wide range of genetic models to disrupt different aspects of dystroglycan protein or glycosylation in forebrain neurons. The authors use a combination of immunohistochemistry and electrophysiology to identify cellular migration, lamination, axonal targeting, synapse formation/function, and seizure phenotypes in forebrain neurons. This is an elegant study with extensive data supporting the conclusions. The role of dystroglycan and the dystrophin glycoprotein complex (DGC) in cellular migration and synapse formation are of broad interest.*
>
> *• A strength of this paper is the use of several transgenic mouse lines with mutations in genes involved in glycosylation of dystroglycan. Knockout of POMT2 abolishes the majority of dystroglycan glycosylation, while point mutations in B4GAT and FKRP presumably produce more minor changes in glycosylation. This is a powerful approach to inves5gate the role of glycosylation in dystroglycan function. However, the authors do not address how mutations in these genes may affect glycosylation or expression of proteins other than dystroglycan. It is possible, even likely, that some of the phenotypes observed are due to changing glycosylation in any number of other proteins. The paper would be strengthened by addressing this possibility more directly.*

We are glad to see that the reviewer appreciated the range of transgenic models used to define the role of Dag1 glycosylation. It is certainly possible that glycosylation of proteins other than Dag1 is affected by deletion of Pomt2, B4Gat1 and/or FKRP. Indeed, Cadherin and Plexin proteins undergo Omannosylation in the brain. However, recent work has shown that

these proteins are not dependent on Pomt1/2 for their O-mannosylation, and use an alternative glycosylation pathway. Therefore, they unlikely to contribute to the phenotypes we observed in our Pomt2, B4Gat1 and/or FKRP mutants. Furthermore, we did not observe any phenotypes in these models that was not also observed in the Dag1 conditional knockouts. We have clarified this point in the results section (lines 117-121) with additional references, and added the caveat that Pomt2, B4gat1, and Fkrp could play a role in the glycosylation of proteins other than Dag1.

> *• It would be helpful to have a more clear description of how dystroglycan glycosylation is altered in B4GAT1M155T or FKRPP448L mice. For example, Figure 1 makes it appear that the distal sugar moieties are missing, however, the IIH6 antibody, which binds to terminal matriglycan repeats on the glycan chain, recognizes dystroglycan in these mutants.*

We apologize for the confusion caused by our schematic in Figure 1. We have adjusted the opacity of the schematic in Figure 1A to better illustrate that the matriglycan chain is s5ll present, albeit at reduced levels, in the B4Gat1 and FKRP mutants. In addition, this is directly shown in the western blot in Figure 1B.

> *• In Figure 1, the authors use the IIH6 antibody, which recognizes the terminal portion of the dystroglycan glycan chain, to label dystroglycan in the hippocampus. As expected, Emx1Cre,POMT2cKO mice, which lack glycosylation of dystroglycan, do not show any labelling. However, this experiment does not reveal anything about dystroglycan expression, only that the IIH6 antibody no longer recognizes dystroglycan. It would be very helpful in interpreting the later results to know whether the level and pattern of dystroglycan expression is normal or absent in the POMT2cKO mice, perhaps using another antibody that does not target the glycosylated region. For example, figure 3 shows reduced axon targeting to the cell body layer in POMT2cKO, however, it is unclear whether this is due to absence/mislocalization of dystroglycan at the cell surface, or if dystroglycan expression is normal, but glycosylation is directly required for axon targeting.*

Addressed in the “Recommendation for Authors” section below

> *• In Figures 3 and 5, the authors use CB1R labelling to measure axon targeting and synapses formation. However, it is not clear how the authors measure axon targeting and synapses number separately using the same CB1R antibody. In addition, figure 3 shows reduced CB1R labelling in Dag1cyto pyramidal cell layer, but Figure 5 shows no change in CB1R labelling in the same mice. These results would appear to be contradictory.*

In Figure 3, the data reflects fluorescent intensity of CB1R+ axons measured across the en5re hippocampal depth. In contrast, the synapse number in Figure 5 is measured as VGat+ and CB1R+ puncta (axonal swellings) within the pyramidal cell layer (SP). The discrepancy between these measurements in the Dag1Cyto mutants likely reflects a change in the distribution of the synaptic contacts in SP (ie: increased contacts in the upper portion of the SP relative to the bottom). This is clarified in the text, lines 315-319.

> *• The authors measure spontaneous IPSCs (sIPSC) in CA1 pyramidal neurons to measure inhibitory synaptic function. This measure assesses inhibitory synaptic input from all sources, but dystroglycan mutations primarily impairs synapses arising from CCK+/CB1R interneurons, leaving synapses arising from PV or other interneurons relatively unchanged. To assess changes in CCK+/CB1R interneurons the authors apply the cholinergic receptor agonist Carbachol (which selectively activates CCK+/CB1R*

interneurons) and measure the change in sIPSC amplitude and frequency. While this is an interesting and reasonable experiment, the observed effects could be due to altered carbachol sensitivity in the transgenic mice. Control experiments showing that the effect of Carbachol on excitability of CCK+/CB1R interneurons is similar across mouse lines is missing.

The reviewer is correct that we did not show that CCK/CB1R+ interneurons have the same sensitivity to CCh in controls and the various mutants. Indeed, this is something we have struggled with over the course of the study, and is an inherent limitation of the current study. Unfortunately, these cells are relatively sparse in the CA1, and therefore patching onto presumptive CCK/CB1R+ INs at random to test this directly is not feasible. There are also no genetic or viral tools that we are aware of at this time to fluorescently label these cells for targeted recordings (this would need to be a Cre-independent transgenic mouse line since we are using Cre to delete Dag1 and Pomt2). We tried to assess this by measuring c-fos immunohistochemistry staining as a proxy for activity in response to CCh. Briefly, we incubated acute slices with NBQX, SR95531, and Kynurenic Acid to block synaptic activity, and added CCh in the bath for 30, 60, and 90 minutes to induce CCK/CB1R+ INs firing. Slices were then fixed and stained for c-fos and NECAB1 to identify the CCK/CB1R+ interneurons.

Unfortunately, we had a very difficult time imaging these slices, and we were not confident in our ability to localize c-fos+/NECAB1+ cells. We have clarified that this is an inherent limitation to the study in the text, lines 394-396.

• Earlier work has shown that selective deletion of dystroglycan from pyramidal neurons produces near complete loss of CCK+/CB1R interneurons and synapse formation, a more severe deficit than observed here using a more widespread Cre-driver. This finding is surprising, as generally more wide-spread gene deletion results in more severe, not less severe, phenotypes. The authors make the reasonable claim that more wide-spread gene deletion better mimics human pathologies. However, possible speculation on why this is the case for dystroglycan could provide insight into the nature of CNS deficits in different forms of dystroglycanopathies.

The reviewer is correct that previous work from both our lab and others have shown that deletion of Dag1 from only pyramidal neurons with NEX-cre leads to a complete loss of CCK/CB1R+ INs, and is thus more severe than the phenotype seen with the broader deletion of Dag1 with Emx1-Cre. We were also surprised by this result, so we also generated Dag1;Nestin-Cre mice. These mice show an iden5cal phenotype as the Dag1;Emx1-Cre mutants (new data; Figure 3, Supplement 1; text lines 226-233). This makes us confident in the validity of the Dag1;Emx-Cre mutants with regards to modeling the human disease. We do not know why the NEX-Cre line shows a more severe phenotype; it is possible that this is due to an unknown epistatic interaction between Dag1 and NEX-Cre.

Reviewer #2 (Public Review):

The manuscript by Jahncke and colleagues is centered on the CCK+ synaptic defects that are a consequence of Dystroglycanopathy and/or impaired dystroglycan-related protein function. The authors use conditional mouse models for Dag1 and Pomt2 to ablate their function in mouse forebrain neurons and demonstrate significant impairment of CCK+/CB1R+ interneuron (IN) development in addition to being prone to seizures. Mice lacking the intracellular domain of Dystroglycan have milder defects, but impaired CCK+/CB1R+ IN axon targeting. The authors conclude that the milder dystroglycanopathy is due to the par5ally reduced glycosylation that occurs in the milder mouse models as opposed to the more severe Pomt2 models. Additionally, the authors postulate that inhibitory synaptic defects and elevated seizure susceptibility are hallmarks of severe

> *dystroglycanopathy and are required for the organization of functional inhibitory synapse assembly.*
>
> *The manuscript is overall, fairly well-written and the description of the phenotypic impact of disruption of Dystroglycan forebrain neurons (and similar glycosyltransferase pathway proteins) demonstrate impairment in axon targeting and organization.*

There are some questions with regards to interpretation of some of the results from these conditional mouse models.

> *• The study is mostly descriptive, and some validation of subunits of the dystroglycanglycoprotein complex and laminin interactions would go towards defining the impact of disruption of dystroglycan's function in the brain.*

Addressed in the “Recommendation for Authors” section below

> *• The statistics and basic analysis of the manuscript appear to be appropriate and within parameters for a study of this nature.*
>
> *• Some clarification between the discrepancies between the Walker Warburg Syndrome (WWS) patient phenotypes and those observed in these conditional mouse models is warranted. This manuscript has the potential to be impactful in the Dystroglycanopathy and general neurobiology fields.*

Addressed in the “Recommendation for Authors” section below

> ***Reviewer #3 (Public Review):***
>
> *The study presents a systematic analysis of how a range of dystroglycan mutations alter CCK/CB1 axonal targeting and inhibition in hippocampal CA1 and impact seizure susceptibility. The study follows up on prior literature identifying a role for dystroglycan in CCK/CB1 synapse formation. The careful assay includes comparison of 5 distinct dystroglycan mutation types known to be associated with varying degrees of muscular dystrophy phenotypes: a forebrain specific Dag1 knockout in excitatory neurons at 10.5, a forebrain specific knockout of the glycosyltransferase enzyme in excitatory neurons, mice with deletion of the intracellular domain of beta-Dag1 and 2 lines with missense mutations with milder phenotypes. They show that forebrain glutamatergic deletion of Dag1 or glycosyltransferase alters cortical lamination while lamination is preserved in mice with deletion of the intracellular domain or missense mutation.*

The study extends prior works by identifying that forebrain deletion of Dag1 or glycosyltransferase in excitatory neurons impairs CCK/CB1 and not PV axonal targeting and CB1 basket formation around CA1 pyramidal cells. Mice with deletion of the intracellular domain or missense mutation show limited reductions in CCK/CB1 fibers in CA1. Carbachol enhancement of CA1 IPSCs was reduced both in forebrain knockouts. Interestingly, carbachol enhancement of CA1 IPSCs was reduced when the intracellular domain of beta-Dag1was deleted, but not I the missense mutations, suggesting a role of the intracellular domain in synapse maintenance. All lines except the missense mutations, showed increased susceptibility to chemically induced behavioral seizures. Together, the study, is carefully designed, well controlled and systematic. The results advance prior findings of the role for dystroglycans in CCK/CB1 innervations of PCs by demonstrating effects of more selective cellular deletions and site specific mutations in extracellular and intracellular domains. The interesting finding that deletion of intracellular domain reduces both CB1 terminals in CA1 and carbachol modulation of IPSCs warrants further analysis. Lack of EEG evaluation of seizure latency is a limitation.

Specific comments

• Whether CCK/CB1 cell numbers in the CA1 are differentially affected in the transgenic mice is not clarified.

This is a good point; we have now addressed this in Figure 3, Supplement 2 (new data; text lines 234-245). In brief, using two different markers (NECAB1 and NECAB2), we see no change in the number of CCK+/CB1R+ INs in the mutant mice.

• 2. Whether basal synaptic inhibition is altered by the changes in CCK innervation is not examined.

We apologize for the confusion. This is addressed in the text, lines 371-375:

"Notably, even baseline sIPSC frequency was reduced in Dag1cyto/- mutants (2.27±1.70 Hz) compared to WT controls (4.46±2.04 Hz, p = 0.002), whereas baseline sIPSC frequencies appeared normal in all other mutants when compared to their respective controls."

Reviewer #1 (Recommendations For The Authors):

Line 321- CCH-mediated CHANGE in sIPSC amplitude...

This has been corrected (now line 356)

Reviewer #2 (Recommendations For The Authors):

Major Comments:

• Disruption of the dystroglycan (and subsequent glycosyltransferase proteins) in the brain would likely impact laminin localization and cytoskeletal stability of the dystroglycanprotein complex. The authors should assess (via immunolabeling) the disruption laminin using laminin IF in the various conditional mouse model forebrain sections.

We have stained brains from Dag1, Pomt2, and Dag1cyto mutants with an antibody to Laminin (new data; Figure 2, Supplement 2; text lines 191-205). Briefly, the data clearly shows that laminin staining is abnormal on the pial surface and in the blood vessels of the Dag1;Emx1-cre mutants. This is less severe in the Pomt2;Emx1 mutants, and normal in the Dag1cyto mutants. We also examined higher magnification of laminin staining in hippocampal SP around the pyramidal cells. Laminin in the region was diffuse (not synaptically localized) and there was no difference between any of the mutants and their respective controls (data not shown).

• 2. The biggest question(s) I have is if the synaptic defects that were measured (Fig 6) in the spontaneous inhibitory post-synaptic currents (sIPSCs) could be rescued as a function of the glycosylation of dystroglycan? While ribitol/CDP-ribose has been shown to enhance alpha-dystroglycan glycosylation and total glycosylation, it might be appropriate here. NADplus exogenous supplementation has been (Ortez-Cordero et al., eLife, 2021) has a faster acting effect on glycosylation of dystroglycan and may work in this context. Can the authors add NADplus prior to their CCK+/CB1R+ IN recordings and evaluate synaptic current effects to determine if glycosylation rescue can actually occur?

We are very much interested in the potential to rescue synaptic defects in the various mutants, and this is an active area of study for us going forward. However, we do not think the suggested experiments involving ribitol/NADplus supplementation are likely to work in

our specific experiments with these models. In Dag1;Emx1-Cre and Pomt2;Emx1-Cre mice, which show the most dramatic phenotype, there is no O-mannosyl chain ini5ated for ribitol to act upon. In the Dag1Cyto mice, matriglycan is normal and therefore ribitol supplementation is unlikely to have an effect. In B4Gat1 and FKRP mutants, while matriglycan is reduced, there is no significant functional synaptic defect observed. Therefore, even if ribitol was able to increase matriglycan in these two mutants, we would be unable to detect a functional difference. As a side note, while the NADplus supplementation is an interesting idea, the previous study cited did these experiments in vitro in cell lines, so it is not clear if this would have the same effect in vivo. In addition, the time frame that they analyzed was following 24-72 hours of supplementation in cultured cells, which led to ~10% increase in IIH6 at 24 hours. We are unable to incubate acute slices for that amount of time prior to our recordings.

> *• 3. Minor point. Genetic abbreviation for POMT2 should be "Pomt2", unless some other justification is provided by the authors. I believe the other mutations introduced (e.g. FKRP P448L are humanized mutations).*

This has been corrected throughout

> *• 4. While dystroglycan glycosylation using the IIHC6 antibody is important for proper localization, the core DAG-6F4 monocloncal antibody (DSHB Iowa Hybridoma Bank) would inform you if there is actual disruption in the amount of dystroglycan protein translation and/or production in the forebrain. Can the authors address this question on total dystroglycan production?*

This is a great suggestion. We obtained both the DAG-6F4 monoclonal antibody from DSHB and a monoclonal antibody to alpha-Dag1 from Abcam (45-3) and tried using them for immunostaining, but they did not work with brain tissue. However, we were able to use an antibody to beta-Dag1 (Leica, B-DG-CE) for immunostaining. This new data is included in Figure 1, Supplement 2 (text lines 134-140) and shows that as expected, beta-Dag1 is completely gone in Dag1;Emx1-Cre and Dag1Cyto mutants. In the Pomt2;Emx1-Cre mutants, betaDag1 is present but no longer has the punctate appearance consistent with synaptic localization. We have added a section in the discussion expanding on the interpretation of the data, lines 449-462.

> *• 5. Please comment more on the structural changes in the forebrain and the presence or lack thereof cobblestone (e.g. lissencephaly) in the POMT2 mutant mice (and the other dystroglycanopathy models)? There appears to be some discordance with that and the human Walker Warburg Syndrome (WWS) patients.*

The Pomt2;Emx1-cre mutants show a cobblestone phenotype (identical to the Dag1;Emx1-Cre mutants), see Figure 2. This is consistent with these two models having a complete loss of Dag1 function, and therefore modeling the most severe forms of dystroglycanopathy (WWS, MEB). In contrast, the B4Gat1 and FKRP mutants show relatively normal cortical migration because these mutants are hypomorphic and therefore retain some degree of functional Dag1. These two mice model a milder form of dystroglycanopathy. We have clarified this on lines 188-190 and 573-578.

> *• 6. Line 577. Minor typo, statement ended in a comma, versus a period.*

Done

> *• 7. Methods. Please report on the sex of the mice used in the experiments.*

Mice of both sexes were used throughout the study. This has been clarified in the methods section, and we have added information regarding how many mice of each sex were used in each experiment in supplemental table 1

> ***Reviewer #3 (Recommendations For The Authors):***
>
> *Additional Specific Comments,*
>
> *• Although authors include n slice/animals and other details in the methodology, including data as % changes and n (slices/animals) in results will greatly improve the readability.*

We have clarified that only one cell per slice was used for physiological recordings (Figure 6) in the methods section, as CCh does not wash out.

> *• 2. IPSCs are measured as inward currents in high chloride with AMPA blockers which is appropriate. However, Mg was appears to be low (1 mM) in cutting solution. Was this the case in the recording solution. If so, why were NMDA blockers not used.*

To clarify, 10mM Mg was included in the cutting solution, and 1mM Mg was included in the recording solution. When the cell is clamped at -70mV, 1mM Mg2+ is sufficient to block NMDA receptors: haps://www.nature.com/ar5cles/309261a0